SYNTHESIS AND CHARACTERISATION OF POLY(ETHYLENE OXIDE) (PEO)/MALEATED STARCH BLENDS

By

HENG JUE JAN

A project submitted to the Department of Chemical Science

Faculty of Science

Universiti Tunku Abdul Rahman

in partial fulfilment of the requirements for the degree of

Bachelor of Science (Hons) Chemistry

May 2017

ABSTRACT

SYNTHESIS AND CHARACTERISATION OF POLY(ETHYLENE OXIDE) (PEO)/MALEATED STARCH BLENDS

Heng Jue Jan

Sago starch was esterified using maleic anhydride in the presence of pyridine as the catalyst. The presence of an intense absorption band at 1739 cm^{-1} in the Fourier Transform Infrared (FTIR) spectrum of maleated starch indicated the successful incorporation of the maleate group into sago starch. Different compositions of PEO/maleated starch blends were prepared by solution casting technique. The isothermal crystallisation and melting behaviour of PEO in the blends were studied using Differential Scanning Calorimetry (DSC). The degree of crystallinity, X_c of PEO decreased with increasing maleated starch content. The effects of crystallisation temperature and blend composition on the crystallisation rate of PEO in the blends were investigated using the well-known Avrami equation. The equilibrium melting temperatures, T_m° of pure PEO and PEO in the blends were estimated using the Hoffman-Weeks approach. The miscibility of PEO and maleated starch was investigated using the polymer-polymer interaction parameter, χ_{12} based on the Nishi-Wang equation. Negative values of χ_{12} for the PEO/maleated starch blends were obtained. This indicated that the PEO/maleated starch blends were thermodynamically miscible in the melt.

ABSTRAK

Anhidrida maleik digunakan untuk mengubahsuai kanji sagu. Piridina dipilih sebagai pemangkin dalam sintesis ini. Penyerapan yang sengit dapat dilihat pada 1739 cm^{-1} dalam spektrum inframerah (IR) kanji yang telah diubahsuaikan. Adunan polimer yang terdiri daripada poli(etilina oksida) (PEO) dan kanji sagu ester disediakan dengan teknik pelarutan. Siasatan sesuhu penghabluran dan lebur kelakuan PEO dalam campuran ini telah dikaji dengan menggunakan Kalorimeter Pengimbasan Perbezaan (DSC). Darjah penghabluran, X_c didapati menurun dengan peningkatan kandungan kanji sagu ester. Implikasi suhu penghabluran dan komposisi campuran pada kadar penghabluran PEO telah dikaji dengan menggunakan persamaan Avrami yang terkenal. Suhu keseimbangan lebur, T_m° PEO tulen dan PEO dalam campuran telah dianggarkan dengan menggunakan pendekatan Hoffman-Weeks. Penurunan suhu keimbangan lebur PEO digunakan untuk mengira interaksi parameter polimer-polimer, χ_{12} berdasarkan persamaan Nishi-Wang. Nilai-nilai yang negatif bagi χ_{12} menunjukkan bahawa sistem PEO/kanji sagu ester adalah larut.

ACKNOWLEDGEMENT

First of all, I would like to express my sincere gratitude to my supervisor, Dr. Tan Shu Min for providing me advice, guidance, and support throughout my final year project.

Besides, I would like to address my appreciation to the laboratory officers for their help throughout this project. Furthermore, I would like to thank my family members for their unconditional support, both financially and emotionally.

Last but not least, I would like to express my deepest gratitude to Universiti Tunku Abdul Rahman for offering me a comfortable environment and sufficient facilities to carry out my project.

DECLARATION

I hereby declare that the project report is based on my original work except for quotations and citations which have been duly acknowledged. I also declare that it has not been previously or concurrently submitted for any other degree at UTAR or other institutions.

_____

(HENG JUE JAN)

APPROVAL SHEET

This project report entitled "**SYNTHESIS AND CHARACTERISATION OF POLY(ETHYLENE OXIDE) (PEO)/MALEATED STARCH BLENDS**" was prepared by HENG JUE JAN and submitted as partial fulfilment of the requirements for the degree of Bachelor of Science (Hons) Chemistry at Universiti Tunku Abdul Rahman.

Approved by:

_____

(DR. TAN SHU MIN) Date: …….
Supervisor
Department of Chemical Science
Faculty of Science
Universiti Tunku Abdul Rahman

FACULTY OF SCIENCE

UNIVERSITI TUNKU ABDUL RAHMAN

Date: _____

PERMISSION SHEET

It is hereby certified that HENG JUE JAN (ID No: 13ADB02968) has completed this final year project entitled "**SYNTHESIS AND CHARACTERISATION OF POLY(ETHYLENE OXIDE) (PEO)/MALEATED STARCH BLENDS**" under the supervision of **Dr. Tan Shu Min** from the Department of Chemical Science, Faculty of Science.

I hereby give permission to the University to upload the softcopy of my final year project in pdf format into the UTAR Institutional Repository, which may be made accessible to the UTAR community and public.

Yours truly,

_____

(HENG JUE JAN)

TABLE OF CONTENTS

LIST OF TABLES

LIST OF FIGURES

LIST OF ABBREVIATIONS

$1/\gamma$	Stability parameter
χ_{12}	Polymer-polymer interaction parameter
ϕ_1	Volume fraction of PEO
ϕ_2	Volume fraction of maleated starch
AGU	Anhydroglucose unit
c	Concentration of HCl
DDSA	Dodecenyl succinic anhydride
DMSO	Dimethyl sulfoxide
DS	Degree of substitution
DSC	Differential scanning calorimetry
ENR	Epoxidised natural rubber
FTIR	Fourier transform infrared
HCl	Hydrochloric acid
ΔH_{m}	Melting enthalpy of PEO
$\Delta H_{\mathrm{m}}^{\circ}$	Melting enthalpy of 100 % crystalline PEO
IR	Infrared
K_{A}	Overall rate constant of crystallisation
$K_{\mathrm{A}}^{1/n_{\mathrm{A}}}$	Generalised rate constant
KBr	Potassium bromide
K_{g}	Nucleation parameter
m_1	Degree of polymerisation of PEO
m_2	Degree of polymerisation of maleated starch
n_{A}	Avrami exponent

NaOH	Sodium hydroxide
OSA	Octenylsuccinic anhydride
PBSU	Poly(butylene succinate)
PEO	Poly(ethylene oxide)
PHB	Poly(3-hydroxybutyrate)
PLA	Poly(lactic acid)
PnBMA	Poly(*n*-butyl methacrylate)
r^2	Correlation coefficient
rpm	Revolutions per minute
R	Universal gas constant
t	Time taken during the crystallisation process
t_0	Induction period
$t_{0.5}$	Half-time of crystallisation
$t_{0.5}^{-1}$	Reciprocal of half-time of crystallisation
ΔT	Undercooling
T_c	Crystallisation temperature
T_m	Observed melting temperature
T_m°	Equilibrium melting temperature
V_0	Volume of HCl used for native starch
V_1	Volume of HCl used for maleated starch
v_1	Molar volume of PEO
v_2	Molar volume of maleated starch
w_{PEO}	Weight fraction of PEO
W	Mass of sample (native sago starch or maleated starch)
w_{MA}	Weight fraction of maleic anhydride

X_c	Degree of crystallinity
X_t	Degree of conversion at time t

CHAPTER 1

INTRODUCTION

Polymer is a large molecule composed of multiple repeating units called monomers, whereby at least 1000 units are connected by covalent bonds to form a macromolecule (Ravve, 2000). Polymers fall into two major categories, namely synthetic polymers and natural polymers. Synthetic polymers are derived from petroleum. Most of these polymers are based on the chemistry of carbon (Cziple and Marques, 2008). The mechanical properties of synthetic polymers can be altered to suit diverse applications such as plastics, elastomers, fibers, adhesives, foams, and films by modifying certain chemical functional groups (Gunatillake and Adhikari, 2003). Despite the fact that synthetic polymers have grown in popularity due to their easily tailored properties, the production of synthetic polymers requires the utilisation of fossil resources which may one day be depleted.

Natural polymers, on the other hand, are those whose origins are from living organisms. Among the wide varieties of natural polymers, starch and cellulose are the well known resources that have the potential to be employed in the manufacture of biodegradable plastics (John and Thomas, 2012). Starch, for instance, is a condensation polymer built up by covalently joining glucose monomers, during which water molecules are released. The use of starch in industrial applications has become an attractive alternative for future materials due to its renewable resources, ample supply, low cost, and ability to impart functional characteristics to different types of products. Furthermore, the

biodegradability of starch helps to overcome issues such as environmental complications, recycling limitations, and fossil resources depletion. However, the hydrophilic nature of starch causes it to have low mechanical properties, thus resulting in a decrease in the durability of starch-based materials (Bertolini, 2009).

Modification of starch emerges as a solution to improve the properties of starch so as to expand its applications in the industrial field. There are two ways of modifying starch, namely chemical modification and physical modification. Chemical modification involves esterification of starch such as acetylation, succinylation, and octenylsuccinic anhydride (OSA) modification. In addition to this, starch can also be subjected to modification using fatty acid derivatives and dicarboxylic acids (Ačkar, et. al., 2015). The extent of modification can be determined using degree of substitution (DS). DS is defined as the average number of hydroxyl (-OH) groups that have been substituted per monosaccharide unit in a polysaccharide (Alger, 1996). In other words, it is a measure of the amount of substituents (Eliasson, 2004).

Physical modification, on the other hand, involves combining two or more polymers together, thus yielding a new material with tailored physical properties known as polymer blend (Chandran, Shanks and Thomas, 2014). Polymer blending is a method involving the physical combination of at least two polymers. The development of polymer blending leads to the generation of new materials with enhanced properties. The resulting polymer blends consist of individual component polymers, each of which experiences little or no loss

of mechanical properties. In this instance, new materials with desired properties can be obtained at lower cost because polymerisation steps are surpassed.

Crystallisation is considered to be a phase transition process that begins with a single-phase system. When the temperature or the pressure of the system is altered, the free energy of the system changes in such a way so that a phase separated state is energetically more favoured (Reiter and Sommer, 2008). In the case of polymers, crystallisation occurs when polymer single crystals are grown from a polymer solution in the form of thin platelets known as lamella. Due to the greater length of the polymer molecules, chain folding occurs. This results in the formation of a crystal structure of high stability. The crystallisation process can also proceed via the phase separation from the polymer melt. In this instance, chains of polymer molecules are oriented to the face of the lamella perpendicularly, thus forcing chain folding to occur (Odian, 2004). The crystallisation and the melting processes in polymers can be investigated using Differential Scanning Calorimetry (DSC).

In this project, sago starch was esterified using maleic anhydride. Pyridine was employed as the catalyst. Polymer blends of poly(ethylene oxide) (PEO) and maleated starch were prepared using solution casting technique. The crystallisation and melting behaviour of PEO in different blend compositions was then investigated using DSC.

The objectives of this project are:

a) To esterify sago starch using maleic anhydride in the presence of pyridine as a catalyst.

b) To confirm the incorporation of maleate group into starch using Fourier Transform Infrared (FTIR) spectroscopy.

c) To determine the degree of substitution (DS) of starch using back-titration method.

d) To study the effect of reaction temperature, amount of pyridine, and amount of maleic anhydride on the DS of starch.

e) To prepare PEO/maleated starch blends by solution casting technique.

f) To investigate the isothermal crystallisation behaviour of PEO in the PEO/maleated starch blends using DSC.

g) To estimate the equilibrium melting temperature, T_m° of PEO in PEO/maleated starch blends.

h) To study the miscibility of PEO and maleated starch based on Nishi-Wang equation.

CHAPTER 2

LITERATURE REVIEW

2.1 Polymer blends

Polymer blending is a method involving the combination of two or more polymers to create new materials whose properties are superior to those of the individual components (Dhevi, Prabu and Pathak, 2014). Depending on their end use, the characteristics of the resulting polymer blends can be manipulated by changing the blend composition and mixing different polymers.

Generally, polymer blends can be categorised into three broad classes, namely miscible polymer blends, immiscible polymer blends, and compatible polymer blends. Since the performance of the end product relies on the miscibility of the blend components, the miscibility determination of polymer blends is of considerable significance (Ren, et. al., 2011). In miscible blends, for instance, homogeneity between the polymers is observed, which in turn leads to an average between the components' mechanical properties. On the other hand, the polymers in immiscible blends experience complete phase separation due to their poor interfacial adhesion, thus causing the resulting polymer blends to have poor mechanical properties (Chandran, Shanks and Thomas, 2014). In order to yield a blend with desired features, it is important to study the properties of the component polymers and their miscibility upon mixing.

Over the years, the development of plastic industry has brought great convenience to the consumers. However, serious environmental pollution problems have also arisen due to the increasing non-biodegradable plastic wastes (Zuo, et. al., 2015). Polymer blending, which involves physically mixing two or more polymers, becomes one of the most effective options to overcome the environmental issues associated to plastic wastes. Natural polymers like starch and cellulose are incorporated as one of the polymers in polymer blends. Polymer blends that are made up of these renewable and biodegradable natural polymers can be degraded naturally in the environment by hydrolysis or enzymatic action of microorganisms, and eventually be decomposed into non-hazardous carbon dioxide and water.

In addition to overcoming environmental complications, polymer blending also emerges as an extremely attractive alternative that possesses a number of influential advantages, especially from an industrial point of view. The synthesis of new polymers is often time-consuming and costly (Thomas, Grohens and Jyotishkumar, 2014). With polymer blending as one of the recourses, polymerisation steps, which are often considered to be tedious, can be surpassed. New materials with enhanced properties can then be prepared at lower cost. For this reason, polymer blends appear to be a potential replacement material for traditional polymers.

2.2 Starches

Starch is a carbohydrate composed of a series of glucose units that are connected by covalent bonds known as glycosidic linkages (Karmakar, Ban and Ghosh, 2014). This naturally occurring polymer is normally stored as granules in most plant cells. In this state, the polymer is most commonly known as native starch (Soto, Urdaneta and Pernia, 2014). Native starch exists in the form of semi-crystalline granules. Generally, starch that is synthesised by plant cells is made up of two polymers of D-glucose, namely amylose and amylopectin. Amylose, which makes up 20 % to 30 % of the native starch, is a lightly branched polymer. The anhydroglucose units in amylose are essentially joined by α-1,4-glycosidic bonds.

On the other hand, amylopectin, which makes up 70 % to 80 % of the native starch, is a highly branched polymer that contains many clusters of short chains (Wang, et. al., 2015). The backbone of amylopectin bears the same structure as amylose, except that it is highly branched at the α-1,6 positions (Alay and Meireles, 2015).

Starch granules may vary in properties, size, and shape, depending on the amounts of amylose and amylopectin present in the starch, as well as the manner in which the two polymers are arranged within the granules (Wang and Copeland, 2013). Figures 2.1 and 2.2 show the molecular structures of amylose and amylopectin, respectively.

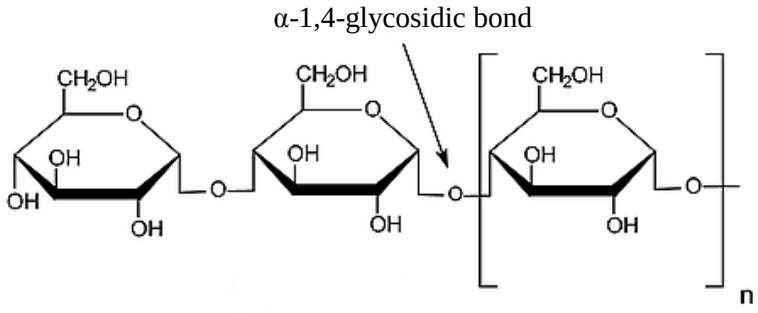

Figure 2.1: Molecular structure of amylose.

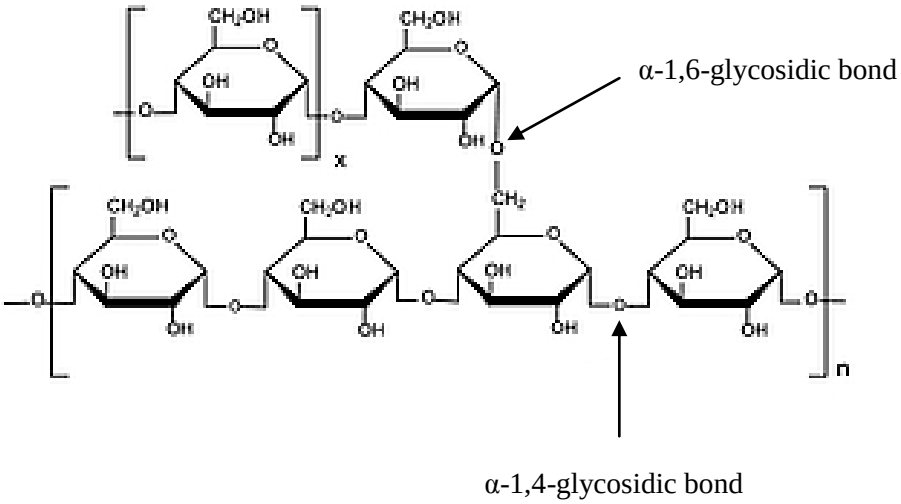

Figure 2.2: Molecular structure of amylopectin.

2.3 Starch modifications

There is no denying that starch has become one of the most sought-after resources to be used in the industry due to their abundant supply, low cost, and ability to impart various functional properties to a wide range of products. Whilst starch possesses a number of attractive properties, there are several property drawbacks that limit the commercial applications of starch. Some of these disadvantages include hydrophilic character of starch, low mechanical properties, and lose viscosity (Ayoub and Rizvi, 2014).

Modification of starch emerges as a resolution to improve the properties of starch so as to expand its industrial applications. Among the various types of modifications available, chemical modification of starch is the most commonly used method because the reaction conditions can be readily manipulated to yield product with desired features. In addition to this, the principal actions and mechanisms of chemical modifications can be well understood compared to other modes of modifications (Fouladi and Nafchi, 2014). Wu, et. al. (2006) reported a successful chemical modification on corn starch by using resorcinol formaldehyde and N-β(aminoethyl)-γ-aminopropyl trimethoxysilane (KH792). The modified corn starch was then used to prepare a starch/styrene butadiene rubber (SBR) composite with reinforced properties.

The susceptibility of starch to modification can be attributed to the presence of three hydroxyl (-OH) groups in each of the anhydroglucose unit in starch (Lewicka, Siemion and Kurcok, 2015). Chemical modification usually involves esterification of starch such as acetylation, succinylation, and octenylsuccinic anhydride (OSA) modification, as well as modification of starch using fatty acid derivatives and dicarboxylic acids (Ačkar, et. al., 2015). The extent of modification can be determined using degree of substitution (DS), an indication of the average number of hydroxyl (-OH) groups that have been substituted per anhydroglucose unit in the starch (Alger, 1996). Since there are three free hydroxyl (-OH) groups present in each of the anhydroglucose unit in starch, the average DS can range from 0 to 3 (Namazi, Fathi and Dadkhah, 2011). Reaction conditions such as pH and temperature can be altered to obtain modified starch products with desired DS.

In a study to incorporate amphiphilic side chains into starch, Chi, et. al. (2007) carried out a modification on corn starch using dodecenyl succinic anhydride (DDSA) *via* base-catalysed reaction. The reaction yielded an esterified starch with a DS of 0.0256. The DS of starch increased with increasing DDSA/starch ratio due to the greater opportunities of collisions between the anhydride and the starch granules. Furthermore, it was found that the DS of starch increased with increasing reaction temperature. This is because an increase in the reaction temperature enhanced the solubility of DDSA in the aqueous phase, thus leading to a greater diffusion of DDSA into the starch granules. This in turn, led to an increase in the rate of the esterification reaction. The infrared (IR) spectrum of the modified starch showed a characteristic band at 1724 cm^{-1} that corresponded to the stretch ester carbonyl group of DDSA. This result confirmed that DDSA has been successfully introduced into the starch backbone.

In a study to investigate the catalytic activity of iodine on the acetylation of corn starch, Diop, et. al. (2011) reported an increase in the DS of starch with increasing concentration of iodine. In this study, acetic anhydride was employed as an esterifying agent. In the presence of iodine as a catalyst, the activation of the carbonyl carbon of acetic anhydride was facilitated. This increased the susceptibility of the carbonyl carbon towards the nucleophilic attack by the hydroxyl (-OH) group on starch, which in turn increased the rate of the esterification reaction. The incorporation of the acetyl group into the corn starch was confirmed by Fourier Transform Infrared (FTIR) spectroscopy.

The emergence of new absorption bands around 1750 cm^{-1}, 1435 cm^{-1}, 1373 cm^{-1}, and 1240 cm^{-1} indicated that the starch was successfully acetylated.

2.4 Poly(ethylene oxide) (PEO)

Poly(ethylene oxide) (PEO) is a low-toxicity polymer produced by the ring opening polymerisation of ethylene oxide. The structural unit of PEO is shown in Figure 2.3.

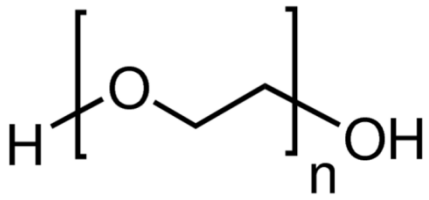

Figure 2.3: Chemical structure of PEO repeating unit.

PEO is a hydrophilic polymer that exhibits high water solubility at room temperature (Back and Schmitt, 2004). Due to its complete solubility in water and low toxicity, PEO is often employed in various pharmaceutical and biomedical applications.

PEO is well known for its thermoplasticity. Thermoplastics are composed of long chains of molecules that are entangled but not interconnected to one another. The chains may be linear or branched (Askeland and Wright, 2015). Thermoplastics can be easily melted upon heating and formed into useful shapes. This allows those with high molecular weight to be readily molded and extruded using conventional thermoplastic equipment.

Films of PEO are capable to withstand stress. Over the years, polymer blends involving PEO have been widely investigated by researchers. PEO are found to be compatible with a number of polymers such as poly(lactic acid), poly(methyl methacrylate), poly(3-hydroxybutyrate), and poly(vinyl chloride).

Biodegradable polymer blends of poly(3-hydroxybutyrate) (PHB) and PEO were prepared by Park, et. al. (2001). PHB is a biodegradable polymer that is highly desirable due to its potential to reduce environmental pollution caused by synthetic polymer waste. However, PHB is stiff and brittle. These characteristics narrow the processability of the polymer itself and lower the polymer's impact strength. In order to overcome the disadvantages associated to the properties of PHB, polymer blend technique was applied, whereby PEO with excellent biocompatibility with PHB was selected. The values of the polymer-polymer interaction parameter obtained using vapour sorption technique were found to be negative for PHB/PEO blends in the whole composition range studied. This suggested that the PHB/PEO blend system was miscible.

Depending on the end uses of a material, PEO can often be blended with various polymers so that their properties are complementary to each other. For instance, polymer blends comprising PEO and epoxidised natural rubber (ENR) were prepared and analysed by Nawawi, Sim and Chan (2012). Despite being a water-soluble thermoplastic that possesses moderate tensile strength and good mechanical property, PEO is a crystalline polymer with high degree of crystallinity. It was reported that this property of PEO exerts a negative

effect on its ionic conductivity. The blending of PEO with ENR appeared to be an alternative for improving the ionic conductivity of the system. The miscibility of the PEO/ENR blend was evaluated using Differential Scanning Calorimetry (DSC). Two glass transition temperatures were obtained for the entire composition range studied. This indicated that the system was immiscible.

2.5 Crystallisation behaviour of polymer blends

Studies related to the crystallisation kinetics of polymer blends are of great significance for their processing-property correlation assessment, owing to the fact that the resulting mechanical properties of the blends are markedly dependent on the degree of crystallinity and the morphology formed (Kalkar and Deshpande, 2001; Zou, et. al., 2011). The conditions during molding, as well as the relative crystallisation times and the extent of crystallisation occurring during processing will influence the morphology of the blend. Factors such as composition of the blend and the order of dispersion achieved during blending contribute to the kinetics of crystallisation. In addition to these, the melting and crystallisation temperatures of the blend components also exhibit a great influence on the development of crystallinity.

Generally, crystallisation begins with a single-phase system. When the temperature or the pressure of the single-phase system is manipulated, the free energy of the system changes in such a way so that a phase separated state is thermodynamically more favoured (Reiter and Sommer, 2008). The result of

this is the primary nucleation of a new phase from the melt polymer, followed by a three-dimensional growth (Freire, et. al., 2012). These two successive events serve as driving forces for the formation of crystals. Secondary nucleation occurs when the existing crystals come into contact with each other, therefore initiating crystal growth. This process often proceeds at a slower rate compared to primary nucleation (Ikehara and Nishi, 2000). However, it is important to recognise the significance of secondary nucleation in establishing the final degree of crystallinity (Chen, Hay and Jenkins, 2013).

2.5.1 Isothermal crystallisation of polymer blends

The kinetics of isothermal crystallisation in polymer blends has been widely investigated by many researchers using DSC, a useful tool in monitoring the progress of crystallisation. In isothermal crystallisation, the sample from the melt is quenched to the crystallisation temperature. Measurement is then made on the heat evolved while the sample is held isothermally (Foreman and Blaine, 1995).

The Avrami equation is applied extensively in the investigation of the polymer crystallisation behaviour under isothermal conditions. This particular equation expresses the volume fraction of crystalline material as a function of time. Two key kinetic events are taken into consideration during the derivation of the Avrami equation – the rate of nucleation and the volume increase in the lamellar crystals (Chuah, Gan and Chee, 1998). In isothermal crystallisation, the onset of crystallisation is employed as a reference zero time (Kalkar and

Deshpande, 2001). However, between the actual beginning of the nucleation process and the experimental zero-time reference, there exists a time lag known as the induction period. This presents an inaccuracy in the values of the Avrami rate constant and the Avrami exponent. The deviations become more noticeable for long crystallisation times. Despite these imperfections, the Avrami model remains to be a well-accepted analysis for the kinetics of isothermal crystallisation.

The isothermal crystallisation kinetics of poly(lactic acid) (PLA) in PLA/starch blends was studied at different isothermal crystallisation temperatures by Ke and Sun (2003). The half-time of crystallisation, defined as the time needed to reach a total of 50 % crystallinity, was obtained and evaluated using the Avrami model. It was found that the half-time of crystallisation increased with increasing crystallisation temperature. Furthermore, the blends containing starch exhibited higher crystallisation rates compared to pure PLA. This indicated that starch in PLA/starch blend acted as a nucleating agent. Further increase in the content of starch in the blend increased the rate of crystallisation of PLA. For this reason, it was concluded that the crystallisation temperatures and the blend compositions were the key factors that affected the crystallisation behaviour of PLA/starch blends from the melt.

The isothermal crystallisation data obtained was used to establish an Avrami plot. The experimental data was able to fit the Avrami equation very well. However, this was only true for the early part of the conversion. At high

degree of conversion, the experimental data started to show pronounced deviation from the straight line. In spite of the limitation, Ke and Sun (2006) claimed that the Avrami method could still be used to characterise the isothermal behaviour of PLA and its blends with starch.

The isothermal crystallisation behaviour of PEO/poly(*n*-butyl methacrylate) (PnBMA) blends was investigated by Shafee and Ueda (2002). It was observed that the overall rate of crystallisation of PEO decreased with increasing amount of PnBMA in the blends. The half-time of crystallisation increased exponentially with increasing crystallisation temperature for all the blends studied. The isothermal crystallisation data was analysed using the Avrami equation. The average value of the Avrami exponent obtained for pure PEO was 2.5, while an average value of 3.0 was obtained for various PEO/PnBMA blend compositions. It was deduced that the diffusion-controlled growth of the crystalline units experienced a change from two-dimensional to three-dimensional.

2.6 Melting behaviour of polymer blends

Equilibrium melting temperature, T_m° is defined as the melting temperature of lamellar crystals with extended chain conformation and the highest degree of perfection (Chung, Yeh and Hong, 2002). T_m° is one of the most significant parameters characterising a polymer (Papageorgiou and Panayioto, 2011).

A comparative study was performed by Qiu, Ikehara and Nishi (2003) to investigate the miscibility and melting behaviour of neat poly(butylene succinate) (PBSU) and PBSU/PEO blends. In their study, it was found that the incorporation of PEO resulted in a reduction in the equilibrium melting temperature, T_m° of PBSU, whereby the T_m° of PBSU decreased with increasing content of PEO. The equilibrium melting depression of PBSU was utilised to calculate the polymer-polymer interaction parameter, χ_{12} based on the Nishi-Wang equation. A negative value of χ_{12} was obtained, indicating that the PBSU/PEO blends were thermodynamically miscible in the melt.

The influence of cationic starch and hydrophobic starch on the miscibility with PEO was evaluated by Pereira, et. al. (2010) using DSC. The analysis was performed based on the depression in the equilibrium melting temperature, T_m°. Based on the Nishi-Wang equation, a positive value for the polymer-polymer interaction parameter, χ_{12} was obtained for the PEO/cationic starch system, thus suggesting that the system was immiscible. The cationic groups that were grafted onto the starch exhibited intramolecular interactions among themselves. This in turn, disrupted the hydrogen bonding between PEO and the starch, thus contributing to the immiscibility of the system. On the other hand, the PEO/hydrophobic starch system was evaluated to be miscible, given that a negative value was obtained for χ_{12}. The miscibility of the system was contributed by two major interactions. The first being the hydrophilic interactions between the hydroxyl (-OH) groups of starch and the oxygen atom of the ether group of PEO, while the second was the hydrophobic interactions between the hydrophobic segments in the starch chain and the ethyl group in

the PEO repeating units. The combination of these two interactions was responsible for the miscibility of the PEO/hydrophobic starch system.

CHAPTER 3

MATERIALS AND METHODS

3.1 Materials

Poly(ethylene oxide) (PEO) with average molecular weight of 200,000 g/mol was purchased from Sigma-Aldrich. Industrial grade sago starch was obtained from Nee Seng Ngeng & Sons Sago Industries Sdn. Bhd. in Sibu, Sarawak. Maleic anhydride and pyridine were supplied by Merck KGaA. Analytical reagent grade dimethyl sulfoxide (DMSO) was purchased from Fisher Scientific. Isopropyl alcohol was obtained from Systerm Chemicals. Acetone was supplied by Scharlab. Ethanol (95 %) was purchased from HmbG Chemicals. Sodium hydroxide (NaOH) was obtained from R&M Chemicals, while hydrochloric acid (HCl) was supplied by GENE Chemical. All chemicals were used without further purification.

3.2 Methods

3.2.1 Synthesis of maleated starch

A 2.75 g (17.0 mmol of anhydroglucose units or AGU) of sago starch, 0.83 g (0.5 equiv.) of maleic anhydride, 0.68 mL (0.5 equiv.) of pyridine, and 6 mL of DMSO were added to a 100 mL two-necked round-bottom flask and stirred for 10 minutes to form a homogeneous suspension. The reaction mixture was refluxed in an oil bath at 100 ℃ for 45 minutes with stirring. Upon

completion of the reaction, the mixture was cooled to 80 ℃. A 40 mL of isopropyl alcohol was added into the reaction mixture to isolate the product by precipitation. The precipitate was then collected by vacuum filtration and washed three times with isopropyl alcohol so as to remove the excess maleic anhydride. The precipitate was subsequently stirred in 40 mL of acetone for 15 minutes and collected by vacuum filtration. The maleated starch was then dried in an oven at 55 ℃ for 48 hours and kept in a dessicator for further analysis. The same procedure was repeated for different amount of maleic anhydride, pyridine, and reaction temperatures.

3.2.2 Verification of the incorporation of maleate group into sago starch using Fourier Transform Infrared (FTIR) spectroscopy

Fourier transform infrared (FTIR) spectra of native sago starch and maleated starch were obtained from KBr/sample pellets. The pellets were prepared by mixing finely ground solid samples and powdered KBr in the ratio of 1:50. The samples were scanned using a Perkin Elmer Spectrum RX1 FTIR Spectrometer within the wavenumber range of 4000 cm^{-1} to 400 cm^{-1}.

3.2.3 Determination of degree of substitution of starch using back-titration method

A 0.5 g of maleated starch was added into 20 mL of 75 % ethanol. The mixture was warmed in a water bath at 50 ℃ for 30 minutes. The mixture was then allowed to cool slowly to room temperature. A 20 mL of 0.5 M NaOH

was added into the mixture. The mixture was shaken continuously at 60 rpm for 24 hours. The excess alkali in the mixture was titrated with 0.5 M HCl using phenolphthalein as an indicator. The titration was repeated twice. A blank titration was carried out using native sago starch.

3.2.4 Preparation of PEO/maleated starch blends using solution casting technique

PEO/maleated starch blends were prepared using solution casting technique. Maleated starch with the highest degree of substitution was used in the preparation of the blends. Six different blend compositions were prepared in the ratio of 100/0, 90/10, 80/20, 70/30, 60/40, and 50/50. The polymers were dissolved in water to obtain a 3 % w/v solution. For instance, to prepare 50/50 PEO/maleated starch blend, 0.25 g of PEO and 0.25 g of maleated starch were dissolved in water. The blend solution was then warmed in a water bath at 50 ℃ for 30 minutes with constant swirling so as to ensure that the polymers dissolved completely. The blend solution was poured onto a Petri dish and kept in an oven at 45 ℃ for 24 hours to evaporate the solvent. The blend films were kept in a dessicator prior analysis.

3.2.5 Differential scanning calorimetry (DSC) measurements

The isothermal crystallisation and melting behaviour of PEO in the PEO/maleated starch blends were studied using a differential scanning calorimeter (Mettler Toledo DSC823). The instrument was equipped with an

intra-cooler system. Nitrogen gas was used as the purge gas. In order to maintain an inert atmosphere, the instrument cell was flushed with nitrogen gas at a flow rate of 20 mL/min. The instrument was calibrated using pure indium (melting point 156.6 ℃) before performing any thermal analysis. For each anaylsis, fresh samples that weighed between 4.0 mg to 4.5 mg were used. The samples were sealed in aluminium sample pans for each measurement. An empty aluminium sample pan was employed as a reference.

3.2.6 Investigation of the isothermal crystallisation behaviour of pure PEO and PEO in the PEO/maleated starch blends

A temperature program, as depicted in Figure 3.1, was used to investigate the isothermal crystallisation behaviour of pure PEO and PEO in the blends. The sample was first heated from 30 ℃ to 90 ℃ at 20 ℃/min. This temperature, otherwise known as the annealing temperature, was held for 3 minutes in order to remove the thermal history. The sample was then quenched to the desired crystallisation temperatures, T_c with a cooling rate of 20 ℃/min. The range of T_c applied in this study was from 43 ℃ to 50 ℃. The sample was then allowed to crystallise isothermally for a certain period of time. The half-time of crystallisation, $t_{0.5}$ was obtained for the range of T_c studied.

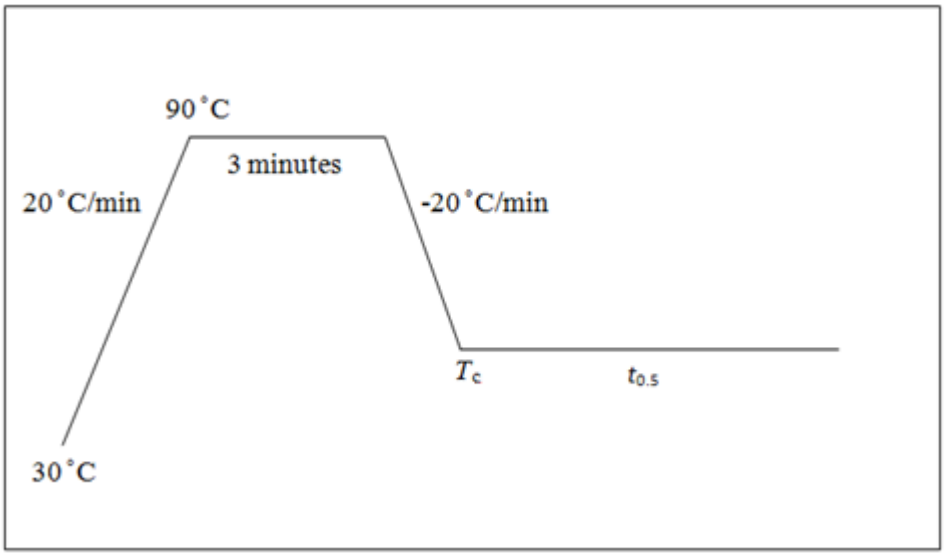

Figure 3.1: Temperature program for isothermal crystallisation measurement at various T_c for pure PEO and polymer blends of PEO/maleated starch.

3.2.7 Estimation of equilibrium melting temperatures, T_m° of pure PEO and PEO in the PEO/maleated starch blends

The melting behaviour of pure PEO and PEO in the blends was estimated by employing a similar temperature program used for isothermal crystallisation measurement. The sample was first heated from 30 ℃ to 90 ℃ at 20 ℃/min. After holding the annealing temperature for 3 minutes, the sample was rapidly cooled to the desired T_c with a cooling rate of 20 ℃/min. The sample was then allowed to crystallise isothermally at different T_c ranging from 45 ℃ to 50 ℃ for five half-times of crystallisation. This was done so as to make sure that the sample crystallised completely. The sample was then heated again to 90 ℃ at the same heating rate. The melting temperatures of pure PEO and PEO in the blends at different crystallisation temperatures were estimated from the first derivative of the melting peak.

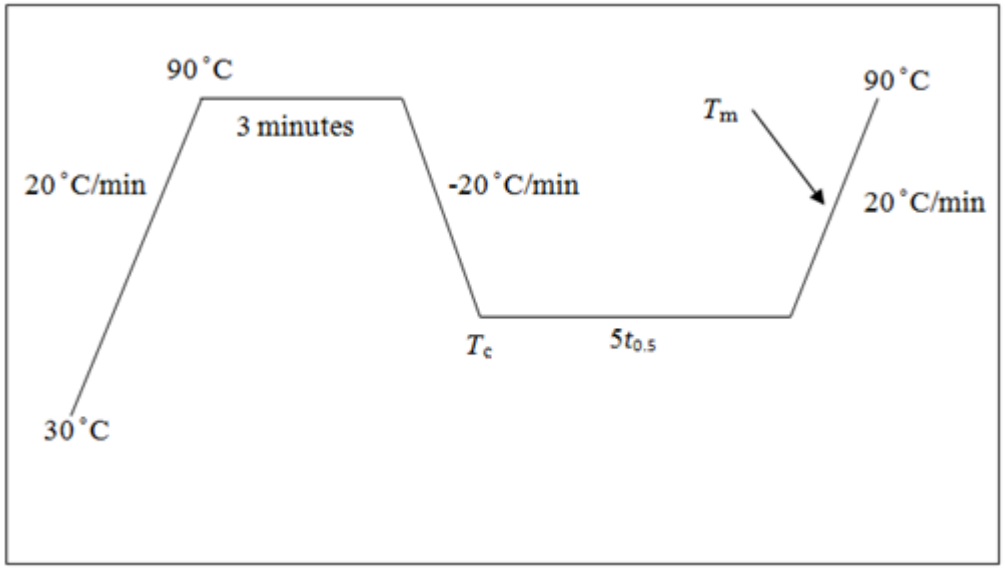

Figure 3.2: Temperature program for melting behaviour study at various T_c for pure PEO and polymer blends of PEO/maleated starch.

CHAPTER 4

RESULTS AND DISCUSSION

4.1 Synthesis of maleated starch

4.1.1 Possible reactions involved in the synthesis of maleated starch

Maleated starch was synthesised by refluxing a mixture of sago starch, maleic anhydride, pyridine, and DMSO at a desired temperature for 45 minutes. Refluxing in pyridine activated the sago starch, thus making it more reactive towards its reaction with maleic anhydride. Besides pyridine, DMSO was also used to aid the substitution of the hydroxyl (-OH) groups in sago starch. Constant agitation of the reaction mixture in the presence of DMSO disrupted the starch granules (Whistler, BeMiller and Paschall, 2012). This allowed the granules to be more susceptible towards maleation.

Pyridine served as a nucleophilic catalyst in the synthesis of maleated starch. The nitrogen atom in the pyridine bears a lone pair of electrons which cannot be delocalised around the ring. This renders nucleophilicity to the molecule, thus making pyridine a suitable reagent to carry out a nucleophilic attack at the carbonyl carbon of maleic anhydride. The carbonyl group was said to be activated by pyridine. The structure of pyridine is depicted in Figure 4.1.

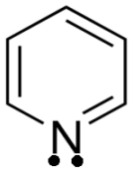

Figure 4.1: Pyridine with its lone pair of electrons.

This activation also resulted in the ring opening of the maleic anhydride. Maleic anhydride, in its activated form, then carried out a nucleophilic attack at the primary hydroxyl (-OH) group on the starch. Figure 4.2 shows the schematic representation of the reaction between sago starch and maleic anhydride.

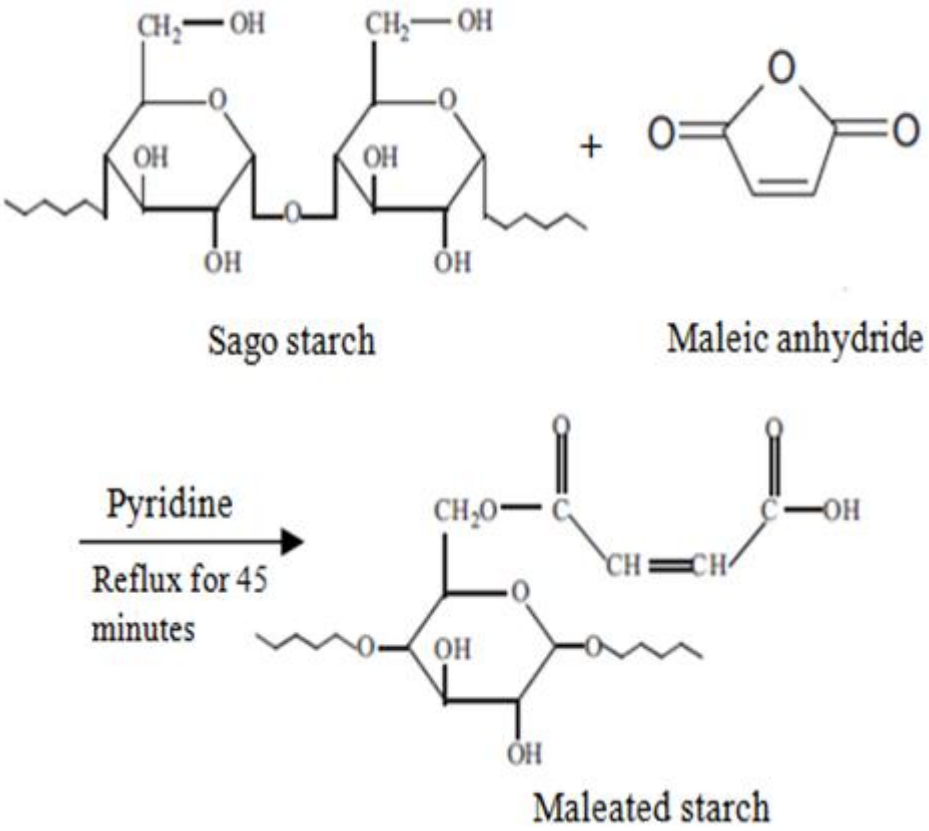

Figure 4.2: Schematic representation of the reaction between sago starch and maleic anhydride.

4.1.2 Verification of the incorporation of maleate group into sago starch using Fourier Transform Infrared (FTIR) spectroscopy

Figure 4.3 shows the comparison of FTIR spectra obtained from native sago starch and maleated starch. Native sago starch showed absorption bands at 1167 cm^{-1} and 984 cm^{-1}. These bands corresponded to the anhydroglucose ring O-C stretch. A characteristic band occurred at 1653 cm^{-1}, which was presumably the H-O bending vibration of the tightly bound water present in the starch (Zuo, et. al., 2013; Kačuráková and Wilson, 2001). An extremely broad band at 3445 cm^{-1} indicated the presence of the hydrogen bonded hydroxyl (-OH) groups. The occurrence of this band was caused by the complex vibrational stretches that were associated to the free, inter- and intra-molecular bound hydroxyl (-OH) groups of the starch chains (Fang, et. al., 2004).

By comparing to the FTIR spectra of the native sago starch, the major change which could be observed from the spectra of the maleated starch was the occurrence of an intense absorption band at 1739 cm^{-1}. This band was attributed to the carbonyl group of the maleate moiety in the maleated starch (Sun and Sun, 2002). This characteristic band served as an indicative of the successful incorporation of the maleate group into sago starch. The bands at 1158 cm^{-1} and 990 cm^{-1} were characteristic of the anhydroglucose ring O-C stretching. The presence of these two bands suggested that there was no ring opening of the anhydroglucose unit during starch maleation (Tay, Pang and Chin, 2012).

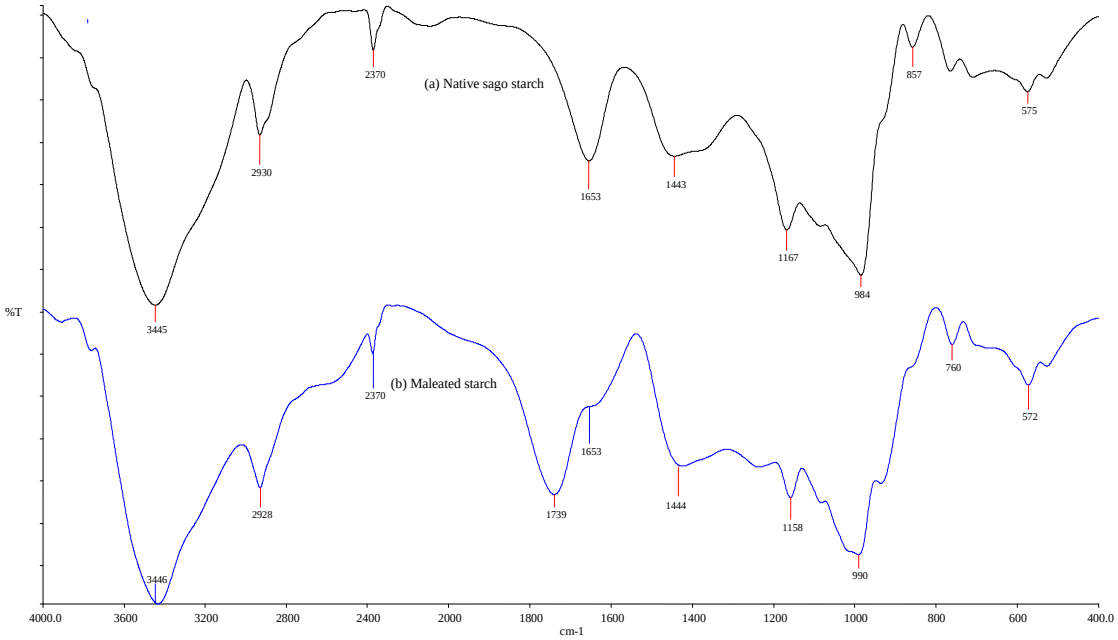

Figure 4.3: FTIR spectra obtained from (a) native sago starch and (b) maleated starch synthesised using 2.0 equiv. of maleic anhydride.

4.1.3 Degree of substitution of starch

Degree of substitution (DS) is defined as the average number of hydroxyl (-OH) groups that have been substituted per anhydroglucose unit in the starch (Alger, 1996). In this study, the carboxyl content of the maleate moiety that was substituted onto the starch chains was utilised to determine the DS of starch (Zuo, et. al., 2013). The percentage of maleate starch with carboxylic end group was determined by dissolving a given amount of sample in a known concentration of NaOH solution. The excess alkali was then back-titrated with HCl. The content of maleic anhydride substituted was determined using Equation (4.1) (Zuo, et. al., 2013):

$$w_{\mathrm{MA}} = \frac{98c(V_0 - V_1)}{1000 \times 2W} \times 100\ \% \qquad (4.1)$$

where w_{MA} is the content of maleic anhydride substituted; c is the concentration of HCl; V_0 and V_1 represent the volume of HCl used for native starch and maleated starch, respectively; W is the mass of the sample; 98 denotes the molar mass of maleic anhydride.

The content of maleic anhydride substituted was then employed in Equation (4.2) (Zuo, et. al., 2013) to determine the DS of starch:

$$\mathrm{DS} = \frac{162 w_{\mathrm{MA}}}{98 \times (100 - w_{\mathrm{MA}})} \tag{4.2}$$

where 162 denotes the molar mass of the anhydroglucose unit in starch.

An attempt was made to study the effects of several reaction parameters on the degree of substitution (DS) of starch. The parameters included the amount of maleic anhydride, amount of pyridine, and various reaction temperatures.

4.1.3.1 Effect of amount of maleic anhydride on DS

Figure 4.4 shows a plot of DS versus amount of maleic anhydride. The reaction was carried out in the presence of various amounts of maleic anhydride and 0.5 equiv. of pyridine. From the plot, it was observed that DS increased with increasing amount of maleic anhydride up to 1.5 equiv. This was due to the greater opportunities of collisions between the anhydride and the starch granules (Chi, et. al., 2007). However, DS started to decrease as the amount of maleic anhydride added was more than 2.0 equiv. This could be attributed to the higher acidity at higher maleic anhydride level. Under this acidic condition, the formation and the hydrolysis of ester both became rapid (Biswas, et. al., 2006). As a result, the net ester formation decreased.

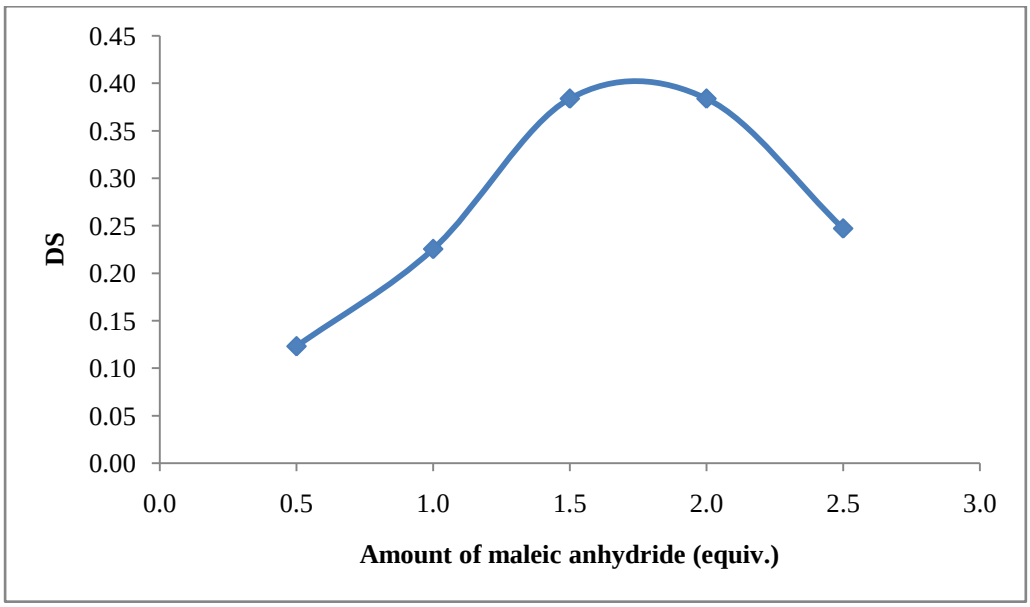

Figure 4.4: Plot of DS versus amount of maleic anhydride.

4.1.3.2 Effect of amount of pyridine on DS

A plot of DS as a function of amount of pyridine is illustrated in Figure 4.5. The reaction was conducted in the presence of different amounts of pyridine and 0.5 equiv. of maleic anhydride. From the plot, it can be seen that the DS increased with increasing amount of pyridine up to 0.6 equiv. As a catalyst, pyridine increased the rate of esterification reaction by providing an alternative pathway with lower activation energy. However, further increase of pyridine amount caused the DS to decrease. It was deduced that extra pyridine slightly hydrolysed the ester.

Biswas, et. al. (2006) conducted an experiment to study the effect of pyridine on the DS of starch. In their study, starch maleate half-esters were prepared using different amounts of pyridine. A similar trend was obtained, whereby the DS of starch increased with increasing amount of pyridine up to 0.5 equiv. The DS started to decrease when the amount of pyridine added was more than 0.5 equiv. This finding, together with the experimental results, implied that pyridine can only serve as a catalyst in an esterification reaction when present in an optimum amount. An excess of pyridine amount will hydrolyse the ester formed.

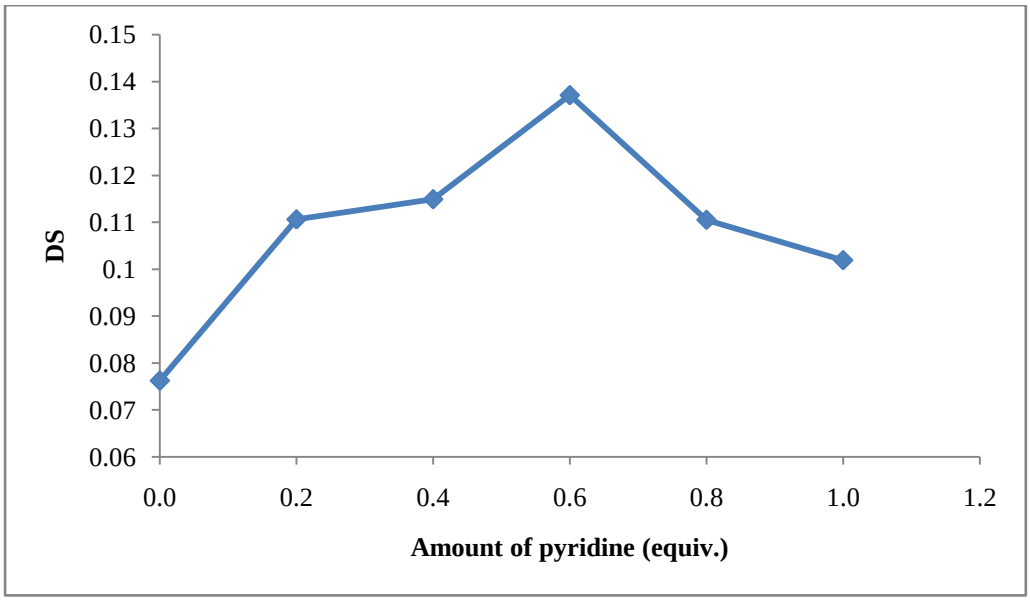

Figure 4.5: Plot of DS versus amount of pyridine.

4.1.3.3 Effect of reaction temperature on DS

Figure 4.6 shows the plot of DS versus reaction temperature. The reaction was carried out using 0.5 equiv. of maleic anhydride at various reaction temperatures without the addition of pyridine and in the presence of 0.5 equiv. of pyridine.

In the absence of pyridine as a catalyst, the DS of starch increased with increasing reaction temperature. As compared to the reaction with pyridine, the DS was always lower for the whole range of reaction temperatures studied. Catalyst served to increase the rate of esterification reaction by providing an alternative mechanism with lower activation energy. Without the catalyst, the esterification reaction has to follow the initial pathway with higher activation energy. Hence, the reaction rate was lowered, thus giving maleated product with lower DS.

With pyridine, the DS of starch increased with increasing reaction temperature up to 80 ℃. This was because elevated temperature easily reached the activation energy needed for the esterification reaction. For this reason, reaction rate was accelerated. Besides, a high reaction temperature increased the rate of collision between the anhydride and the starch granules, thus giving greater opportunities for the esterification reaction to occur. However, the DS remained the same with further increase in temperature.

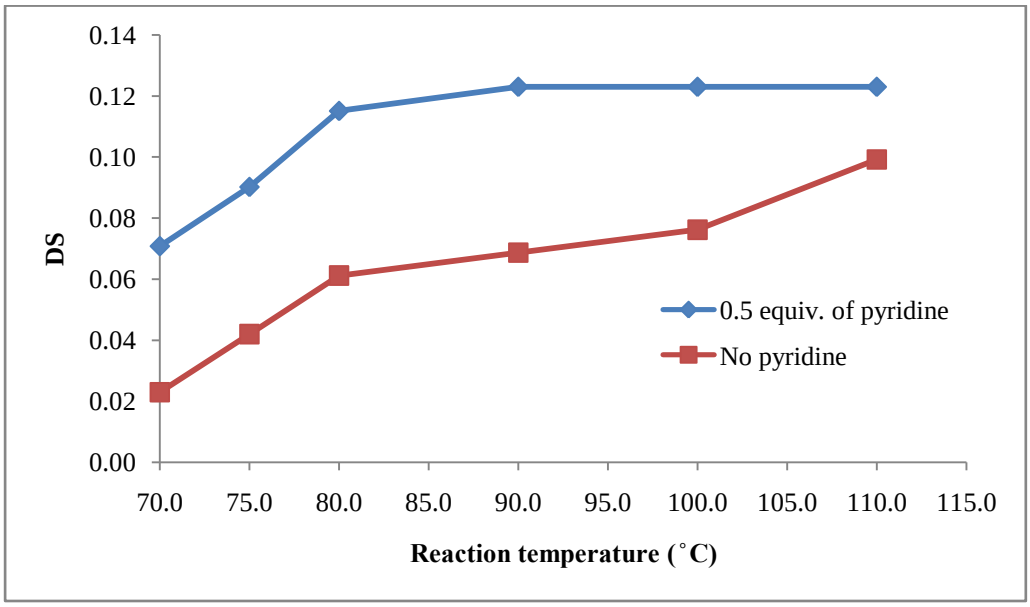

Figure 4.6: Plot of DS versus reaction temperature.

4.2 Differential scanning calorimetry (DSC) measurements

Differential scanning calorimetry (DSC) is a thermoanalytical technique that works according to the heat flow principle. This technique involves measuring the change in the heat flow to the sample and to a reference when they are subjected to a controlled temperature program (Höhne, Hemminger

and Flammersheim, 2013). DSC is often applied in the studies of transitions such as melts, glass transitions, and crystallisation.

4.2.1 Degree of crystallinity, X_c

Polymers in the solid state are composed of two major domains, namely the ordered crystalline domain and the disordered amorphous domain (Brown, et. al., 2008). The relative amounts of crystalline and amorphous regions vary from polymer to polymer. Polymer crystallinity is often determined by DSC, whereby the amount of heat associated to the melting (fusion) of the polymer is quantified (Crompton, 2006). The value can be calculated by dividing the melting enthalpy of the material by the melting enthalpy of 100 % crystalline material. During the calculation, the amount of material is also taken into account so as to determine its effect on the degree of crystallinity of the polymer. In order to determine the degree of crystallinity of PEO, the melting enthalpies of PEO in the blends were obtained from the thermograms. The degree of crystallinity, X_c of PEO was calculated based on Equation (4.3):

$$X_c = \frac{\Delta H_m}{\Delta H_m^\circ \times w_{PEO}} \times 100\ \% \tag{4.3}$$

where ΔH_m denotes the melting enthalpy of PEO in the blend after isothermal crystallisation, J/g; ΔH_m° refers to the melting enthalpy of 100 % crystalline PEO, J/g; w_{PEO} is the weight fraction of PEO in the blend. ΔH_m° was taken to be 196.6 J/g from the literature (Araneda, et. al., 2011). Figure 4.7 shows a plot of the degree of crystallinity, X_c of PEO versus the weight fraction of maleated

starch after isothermal crystallisation at crystallisation temperature, T_c = 46.0 °C.

The degree of crystallinity, X_c of pure PEO was estimated to be 64.5 %. From Figure 4.7, it can be observed that the overall degree of crystallinity of PEO decreased with increasing maleated starch content. This trend could be explained in terms of chain mobility. Sufficient chain mobility serves as a major factor in polymer crystallisation. In comparison with PEO, maleated starch is relatively amorphous. The incorporation of an amorphous component into a blend increased the viscosity of the blend, thus inhibiting chain mobility (Li, 1985). Since the chain mobility of PEO was disrupted by the addition of maleated starch, the degree of crystallinity of PEO decreased.

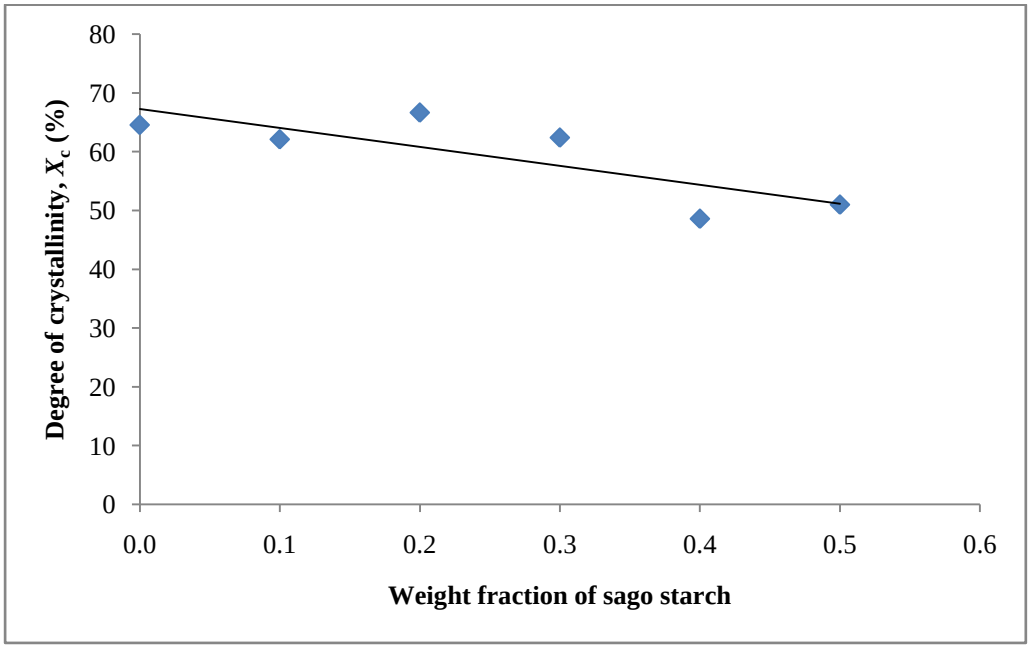

Figure 4.7 Degree of crystallinity, X_c of PEO versus weight fraction of maleated starch at T_c = 46 °C.

4.2.2 Kinetics of isothermal crystallisation

The isothermal crystallisation behaviour of PEO in the PEO/maleated starch blends was investigated at various crystallisation temperatures by using DSC. Figure 4.8 displays a DSC thermogram with a crystallisation exotherm for 60/40 PEO/maleated starch blend at T_c = 44.0 ℃. The induction period, t_0 is indicated in the figure. The area under the exothermic peak can be used to characterise the degree of conversion, X_t. This can be done by integrating the peak area to give the amount of heat released. The equation involved in the determination of X_t is as follows:

$$X_t = \frac{\Delta H_t}{\Delta H_\infty} = \frac{\int_0^t \left(\frac{dH}{dt}\right) dt}{\int_0^\infty \left(\frac{dH}{dt}\right) dt} = \frac{a_t}{a_\infty} \tag{4.4}$$

where ΔH_t and ΔH_∞ denote the heat released at time t and infinite time, respectively; *(dH/dt)* is the heat flow rate of sample; a_t and a_∞ represent the area under the exothermic peak at time t and $t \to \infty$, respectively. The degree of conversion, X_t can therefore be obtained as the ratio of the peak area at time t to the peak area at $t \to \infty$.

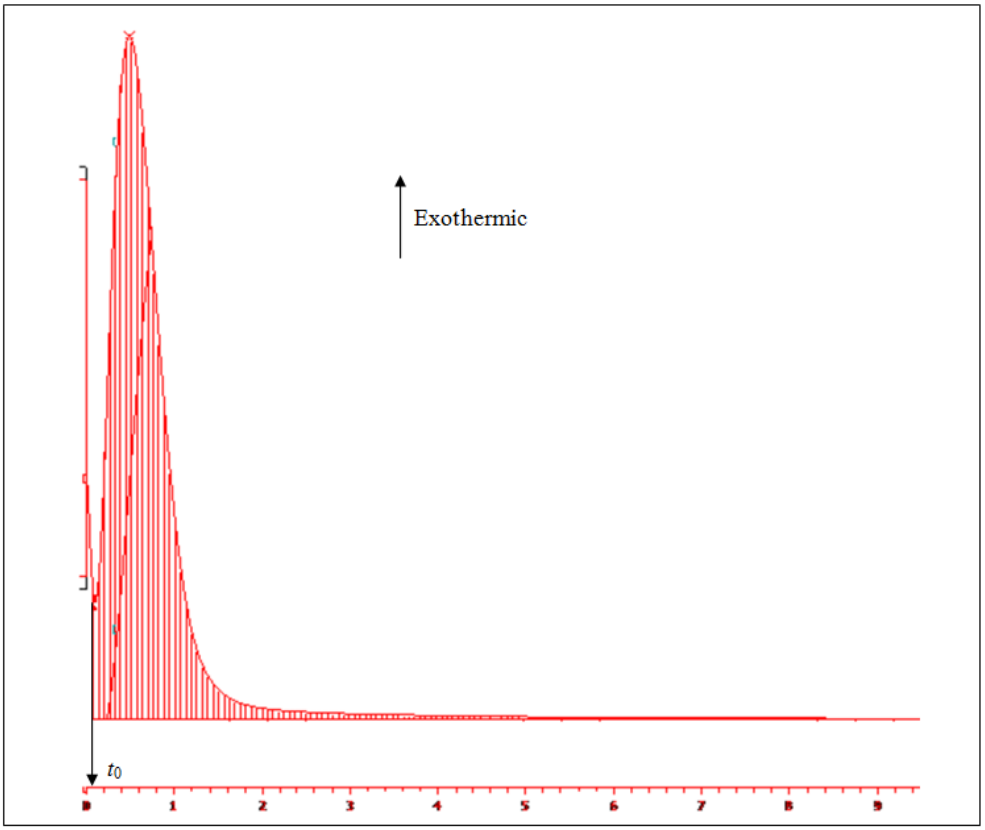

Figure 4.8: DSC thermogram for 60/40 PEO/maleated starch blend at T_c = 44.0˚C.

Avrami equation was used to evaluate the kinetics of isothermal crystallisation of PEO in the PEO/maleated starch blends. Equation (4.5) depicts the well-known Avrami equation:

$$1 - X_t = \exp[-K_A(t - t_0)^{n_A}] \quad (4.5)$$

where X_t represents the degree of conversion at time t; K_A is the overall rate constant of crystallisation, a kinetic parameter which depends on the holding temperature, rate of nucleation, and growth rate; t is the time taken during the crystallisation process; t_0 is the induction period; n_A is the Avrami exponent which reflects the nucleation rate and the growth morphology. By taking

double logarithms on both sides of Equation (4.5), a linearised Avrami equation is obtained. The equation is as follows:

$$\log[-\ln(1 - X_t)] = \log K_A + n_A \log(t - t_0) \qquad (4.6)$$

A straight line with a slope of n_A and an intercept of log K_A can be obtained from the Avrami plot of log[-ln(1 – X_t) versus log(t – t_0).

Figure 4.9 shows some selected Avrami plots of PEO in 50/50 PEO/maleated starch blend at various crystallisation temperatures.

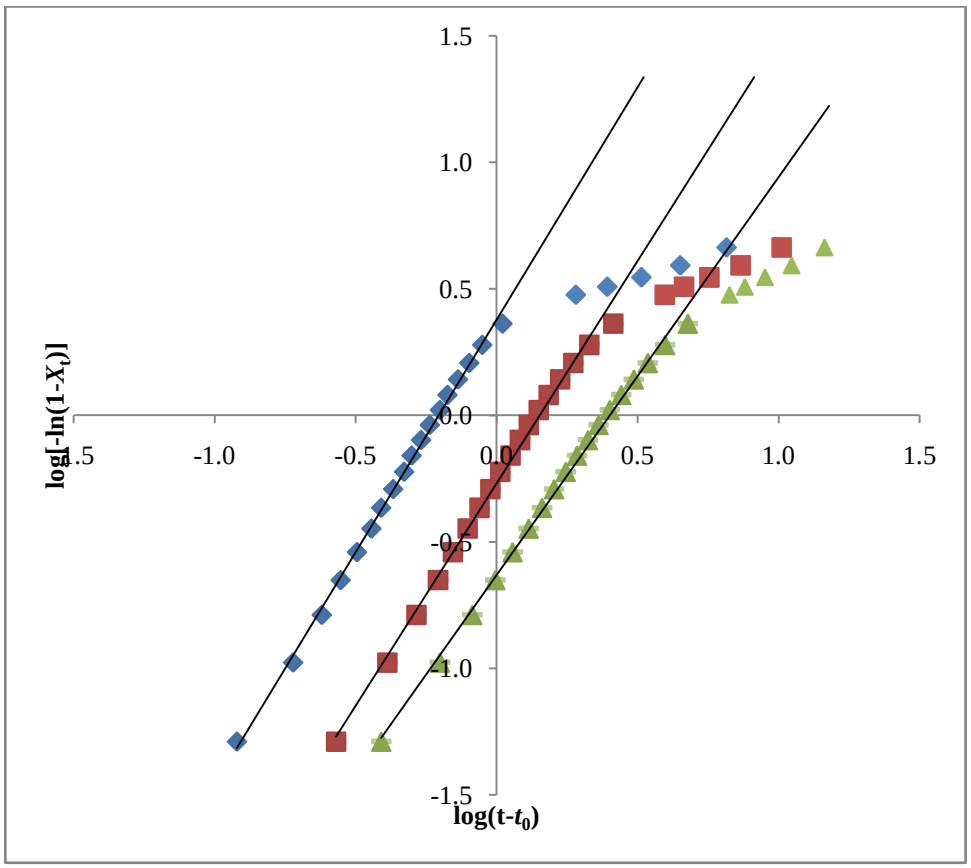

Figure 4.9: Avrami plots of PEO in 50/50 PEO/maleated starch blend at various crystallisation temperatures, T_c. Crystallisation temperatures, T_c: (◆) 44.0˚C, (■) 46.0˚C, (▲) 48.0˚C.

As depicted in the figure, the experimental data was able to fit into the Avrami equation up to 95 % degree of conversion at various crystallisation temperatures. However, deviation from the straight line began to occur beyond 95 % degree of conversion. In general, crystallisation process consists of two stages, namely primary crystallisation and secondary crystallisation. The former resembles the linear portion of the Avrami plot, whereby nuclei are formed from the polymer melt. The latter, on the other hand, refers to the formation of nuclei in the presence of existing crystals. During secondary crystallisation, the crystals grow freely until they start to hit each other. This process, which is known as crystal impingement, interferes with the subsequent nucleation of the crystals (Thakur and Kessler, 2015). This in turn, led to a decrease in the resulting Avrami exponent, thus yielding a non-linear Avrami plot (Sun, Liu and Lu, 1996).

The Avrami parameters for the isothermal crystallisation of PEO in the 50/50 PEO/maleated starch blend are tabulated in Table 4.1. The non-integral values of the Avrami exponent, n_A indicated the presence of the combination of thermal and athermal nucleation and mechanisms (Kalkar, Deshpande and Kulkarni, 2008). The Avrami exponent, n_A obtained for PEO in the blends varied from 1.5 to 2.0, thus suggesting a two-dimensional crystal growth geometry.

Table 4.1: Avrami parameters for isothermal crystallisation of PEO in the 50/50 PEO/maleated starch blend at various crystallisation temperatures.

Crystallisation temperatures, T_c (℃)	Avrami exponent, n_A	Generalised rate constant, K_A^{1/n_A}	Half-time of crystallisation, $t_{0.5}$ (min)	Correlation coefficient, r^2
43.0	1.95	2.33	0.352	0.997
44.0	1.84	1.61	0.500	0.998
45.0	1.68	1.37	0.570	0.996
46.0	1.80	0.71	1.120	0.998
47.0	2.18	0.59	1.390	0.989
48.0	1.57	0.40	1.930	0.997
49.0	1.50	0.19	3.980	0.997
50.0	1.82	0.12	6.862	0.994

Half-time of crystallisation, $t_{0.5}$ is defined as the time required to obtain a total of 50 % crystallinity. Values of $t_{0.5}$ were determined from the area under the crystallisation peak after the induction period, t_0. In this study, the rate of crystallisation at various crystallisation temperatures was expressed in terms of $t_{0.5}$. Figure 4.10 illustrates a plot of half-time of crystallisation, $t_{0.5}$ of PEO versus crystallisation temperature, T_c. At a constant blend composition, the half-time of crystallisation, $t_{0.5}$ increased exponentially with increasing crystallisation temperature, T_c. In other words, the crystallisation rate decreased exponentially with increasing crystallisation temperature, T_c. This phenomenon could be understood in terms of two competing processes, namely molecular transport in the polymer melt (diffusion) and nucleation. Diffusion rate is enhanced at high crystallisation temperatures. Under this condition, the chain mobility of the polymer is so high to the extent where the crystallisation

process is avoided. In this case, nucleation rate is very low (Pereira, et. al., 2010). This in turn, slows down the crystallisation process. The same trend was observed for the whole range of blend compositions studied.

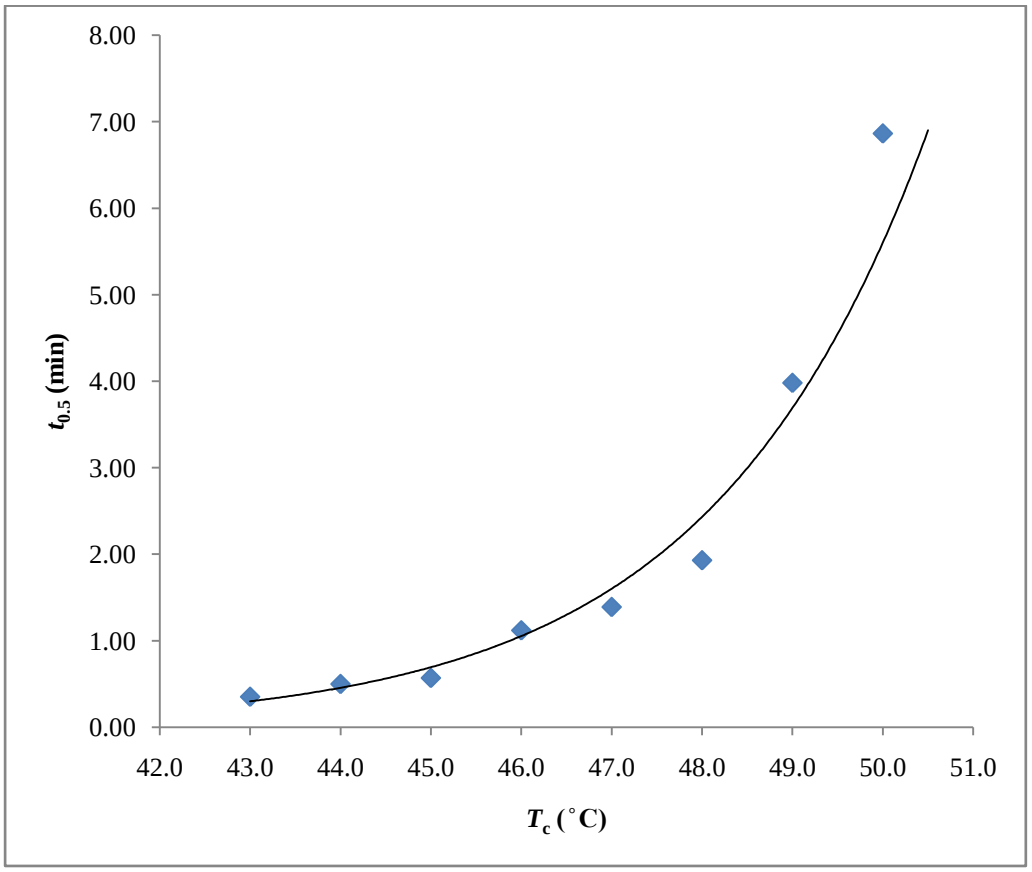

Figure 4.10: Half-time of crystallisation, $t_{0.5}$ of PEO versus crystallisation temperature, T_c for 50/50 PEO/maleated starch blends.

Besides half-time of crystallisation, the rate of crystallisation could also be expressed in terms of generalised rate constant, K_A^{1/n_A}. Values of K_A^{1/n_A} were determined from both the Avrami exponent, n_A and the overall rate constant of crystallisation, K_A. Figure 4.11 shows a plot of generalised rate constant, K_A^{1/n_A} as a function of crystallisation temperature, T_c. From the plot, it was observed that the generalised rate constant, K_A^{1/n_A} decreased exponentially with increasing crystallisation temperature, T_c. This indicated

that the crystallisation rate decreased exponentially with crystallisation temperature, T_c.

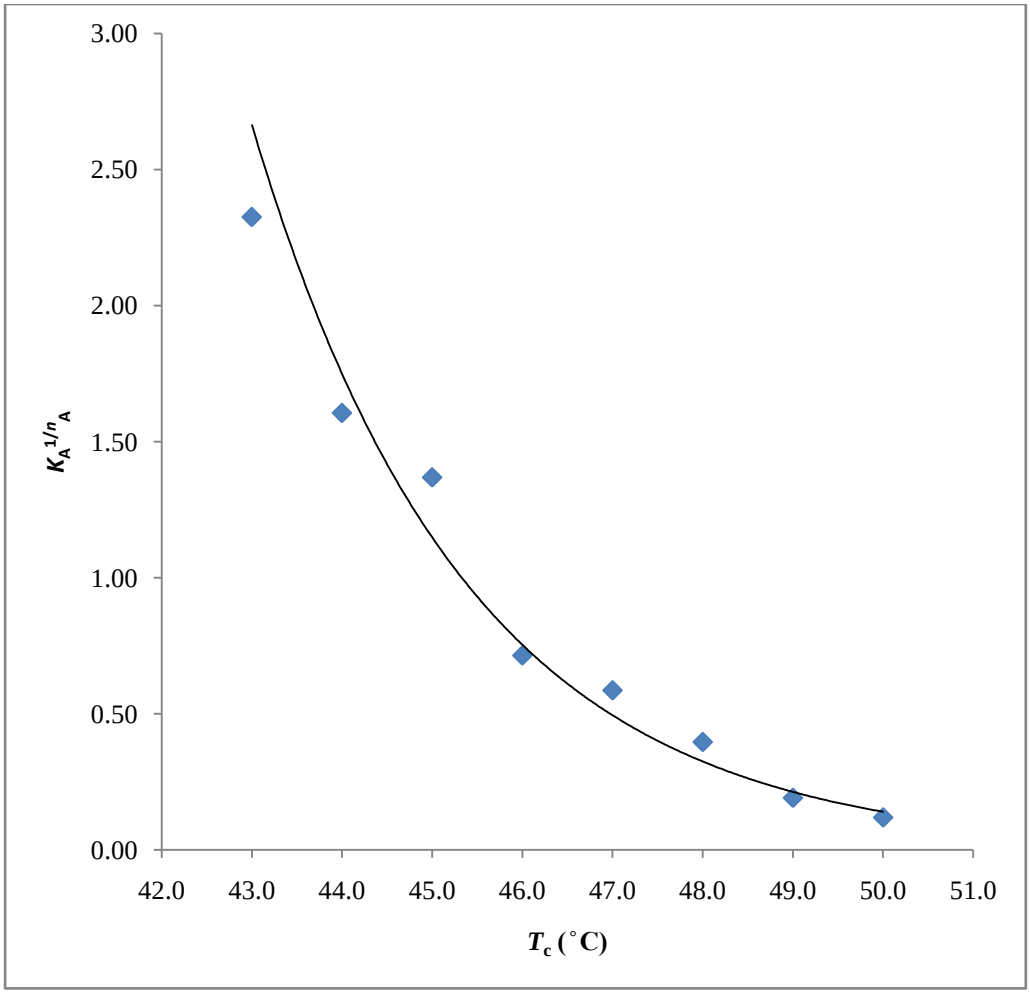

Figure 4.11: Generalised rate constant, K_A^{1/n_A} as a function of crystallisation temperature, T_c for 50/50 PEO/maleated starch blends.

The reciprocal of half-time of crystallisation, $t_{0.5}^{-1}$ can be related to the generalised rate constant, K_A^{1/n_A} . Equation (4.7) shows the relationship between the two parameters:

$$t_{0.5}{}^{-1} = \left(\frac{K_A}{\ln 2}\right)^{1/n_A} \tag{4.7}$$

Figure 4.12 illustrates the logarithmic plot of generalised rate constant, K_A^{1/n_A} versus crystallisation temperature, T_c and the logarithmic plot of reciprocal of half-time of crystallisation, $t_{0.5}^{-1}$ versus crystallisation temperature, T_c. A linear relationship was established for each plot, whereby both log ($t_{0.5}^{-1}$) and log (K_A^{1/n_A}) decreased with increasing crystallisation temperature, T_c. Since the same tendency was observed for both plots, it can be concluded that the crystallisation rate decreased with increasing crystallisation temperature, T_c.

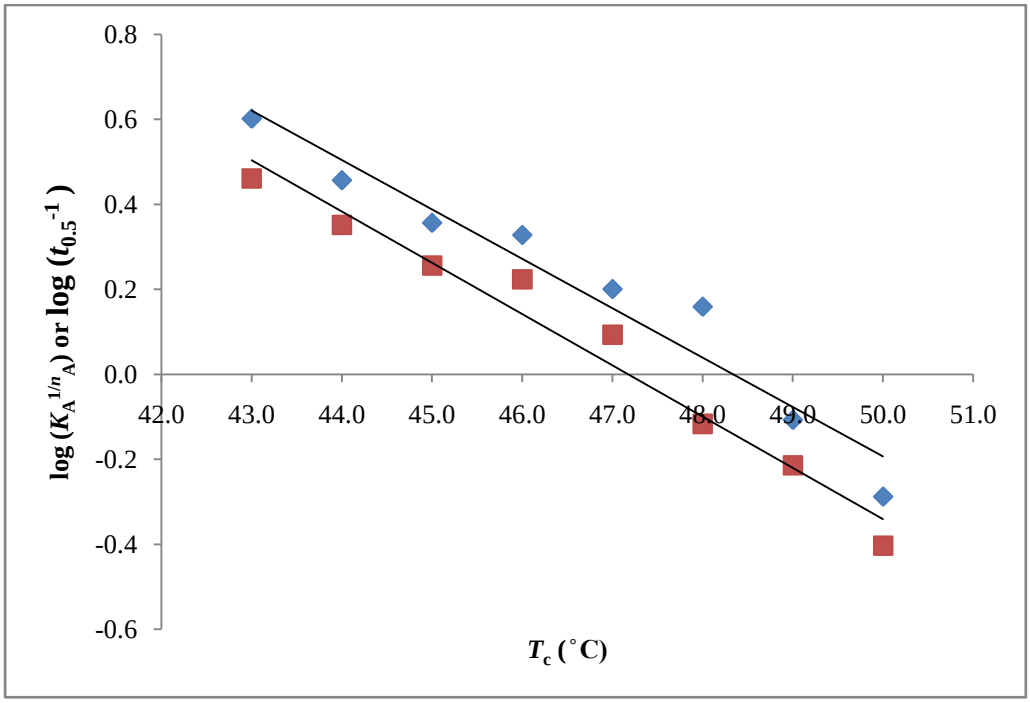

Figure 4.12: Logarithmic plot of generalised rate constant, K_A^{1/n_A} versus crystallisation temperature, T_c and logarithmic plot of reciprocal of half-time of crystallisation, $t_{0.5}^{-1}$ versus crystallisation temperature, T_c for 80/20 PEO/maleated starch blend. (◆) log ($t_{0.5}^{-1}$) and (■) log (K_A^{1/n_A}).

The dependence of crystallisation rate on the weight fraction of maleated starch was studied. Figure 4.13 shows a plot of crystallisation rate as a function of weight fraction of maleated starch. The crystallisation rate was expressed in terms of the reciprocal of half-time of crystallisation, $t_{0.5}^{-1}$.

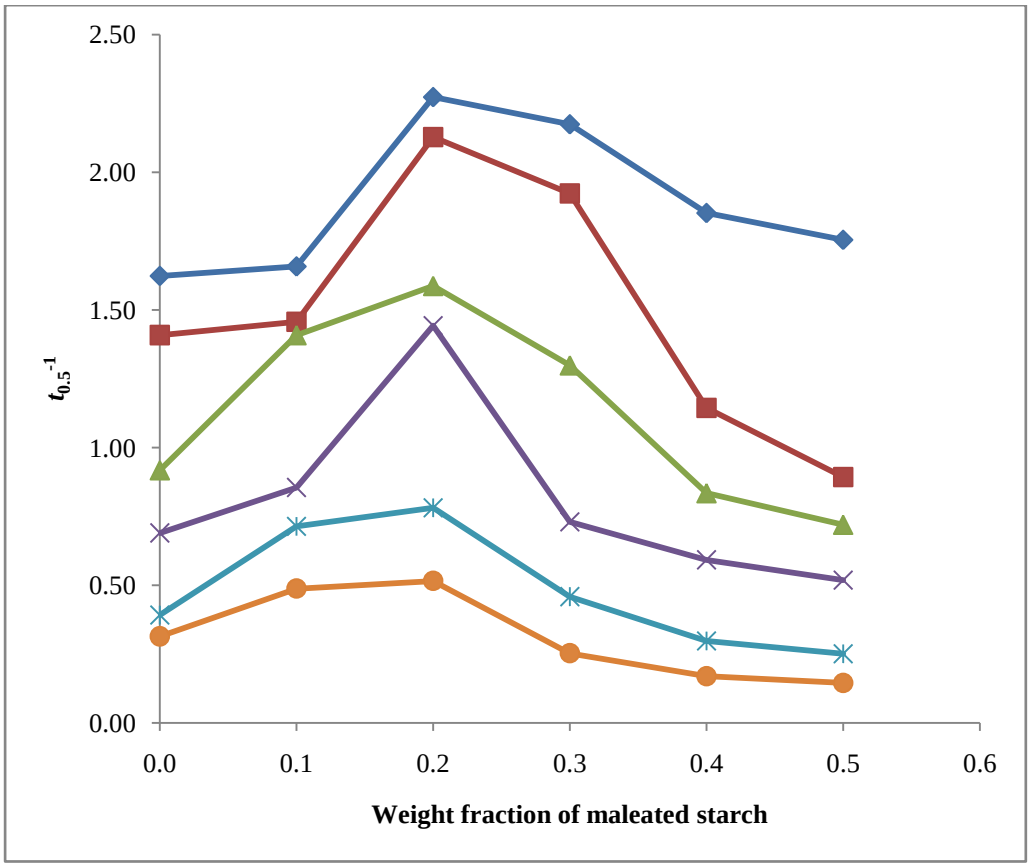

Figure 4.13: Reciprocal of half-time of crystallisation, $t_{0.5}^{-1}$ versus weight fraction of maleated starch for different ratios of PEO/maleated starch blends at a given crystallisation temperature, T_c. Crystallisation temperatures, T_c: (◆) 45.0˚C, (■) 46.0˚C, (▲) 47.0˚C, (✕) 48.0˚C, (✳) 49.0˚C, (●) 50.0˚C.

Based on Figure 4.13, it was observed that the crystallisation rate of PEO in the PEO/maleated starch blend increased with increasing maleated starch content up to 20 %. This was true for the whole range of crystallisation temperatures, T_c studied. The increase in the crystallisation rate could be attributed to the role of maleated starch as a nucleating agent for the lower maleated starch content. The maleated starch formed extremely small nucleus that would act as a nucleating center for the crystallisation of PEO in the blend, thus enhancing the rate of crystallisation (Ke and Sun, 2003). However, the crystallisation rate of PEO in the blend decreased when the amount of maleated starch added was more than 20 %. This phenomenon could be understood in

terms of chain mobility. At high starch content, the viscosity of the blend increased due to the aggregation of the starch granules. This resulted in a decrease in the chain mobility of PEO in the blend, thus inhibiting crystal growth.

In a study conducted by Pereira, et. al. (2004) to investigate the dependence of crystallisation rate of PEO on the weight fraction of cationic starch, a similar trend was obtained. The crystallisation rate of PEO in the PEO/cationic starch blend was found to increase with increasing cationic starch content up to 5 %. When the amount of cationic starch added was more than 5 %, the crystallisation rate started to decrease. The finding corresponded to the experimental data obtained in this study, thus implying that the isothermal crystallisation of PEO in the PEO/maleated starch blend was influenced by the blend composition.

4.2.3 Estimation of equilibrium melting temperatures, T_m° of pure PEO and PEO in the blends

Equilibrium melting temperature, T_m° is defined as the melting temperature of an ensemble of crystals with extended chain conformation and the highest degree of perfection (Chung, Yeh and Hong, 2002). T_m° is especially important in understanding the mechanism of crystallisation. This is because crystallisation phenomena like lateral growth rate and nucleation rate are dependent on the rate of undercooling, $\Delta T = T_m^\circ - T_c$ (Okeda, Ogawa and Matsumoto, 2006), whereby information of both T_m° and T_c are required.

Hoffman-Weeks method is one of the most commonly used approaches in the determination of T_m°. Since only the experimental melting temperature, T_m of the crystallites formed at a certain T_c is required, Hoffman-Weeks method is considered to be a simple procedure that is widely applicable (Soccio, et. al., 2012). In order to estimate the equilibrium melting temperatures, T_m° of pure PEO and PEO in the blends, the samples were first crystallised isothermally for five half-times of crystallisation, $t_{0.5}$ at various crystallisation temperatures, T_c. The observed melting temperatures of pure PEO and PEO in the blends at different crystallisation temperatures were then determined from the first derivative of the melting peak. The Hoffman-Weeks equation, as depicted in Equation (4.8), was then employed to estimate the equilibrium melting temperatures, T_m° of pure PEO and PEO in the blends:

$$T_m = \left(\frac{1}{\gamma}\right) T_c + \left(1 - \frac{1}{\gamma}\right) T_m^\circ \tag{4.8}$$

where $1/\gamma$ refers to the stability parameter that is influenced by the lamellar thickness. The value of $1/\gamma$ varies between 0 and 1. The polymer crystals are considered to be stable when $1/\gamma$ approaches 0 and unstable when $1/\gamma$ approaches 1.

A Hoffman-Weeks plot can be established based on Equation (4.8), whereby T_m is plotted as a function of T_c. The stability parameter, $1/\gamma$ can be estimated from the slope of the plot. By extrapolating the curve of T_m versus T_c to the line $T_m = T_c$, the equilibrium melting temperature, T_m° of a sample can be estimated from the intersection point. Figure 4.14 shows the Hoffman-Weeks

plots for various PEO/maleated starch blends. The equilibrium melting temperature, T_m° of pure PEO was estimated to be 91.2 ℃. The high value of T_m° obtained could be attributed to the high molecular weight of PEO used.

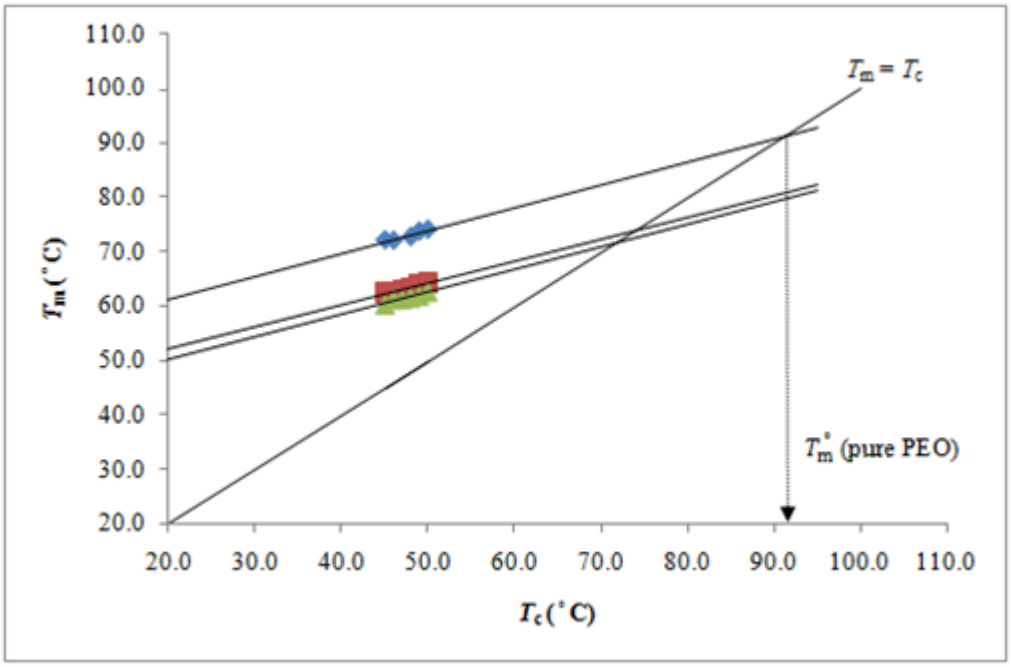

Figure 4.14: Hoffman-Weeks plots for pure PEO, 70/30, and 50/50 PEO/maleated starch blends. Blend compositions: (◆) pure PEO, (■) 70/30, (▲) 50/50.

Table 4.2 shows the equilibrium melting temperatures, T_m° and the stability parameters, 1/γ of pure PEO and PEO in the blends. The stability parameters, 1/γ of pure PEO and PEO in the blends varied from 0.29 to 0.42. The values obtained were close to 0, thus implying the crystals formed were stable. A depression in the equilibrium melting temperatures, T_m° of PEO in the blends was observed. This indicated that the addition of maleated starch in the blend resulted in a decrease in the equilibrium melting temperature, T_m°.

Table 4.2: Equilibrium melting temperatures, T_m° and stability parameters, 1/γ of pure PEO and PEO in the blends.

Blend composition (PEO/maleated starch)	Equilibrium melting temperature, T_m° (℃)	Stability parameter, 1/γ
100/0	91.2	0.4200
80/20	69.1	0.2874
70/30	73.8	0.4006
50/50	71.6	0.4157

4.2.4 Determination of nucleation parameter, K_g for isothermal polymer crystallisation

Nucleation parameter, K_g is regarded as the energy needed to form a secondary nucleus of a critical size (Kocic, et. al., 2015). The value of K_g is often calculated in the investigation of the connection between crystallisation process and morphology of polymers. The relationship between K_g and reciprocal of half-time of crystallisation, $t_{0.5}^{-1}$ can be described as Arrhenius-like. The equation involved in the calculation of K_g is given as follows:

$$t_{0.5}{}^{-1} = \exp\left(-K_g \frac{T_m^\circ}{T_c \Delta T}\right) \tag{4.9}$$

where K_g denotes the nucleation parameter; T_m° is the equilibrium melting temperature of pure PEO, which is 91.2 ℃; ΔT represents undercooling, the value of which can be calculated by subtracting T_c by T_m°. Taking double natural logarithms on both sides of Equation (4.9) gives Equation (4.10):

$$\ln({t_{0.5}}^{-1}) = -K_g \frac{T_m^\circ}{T_c \Delta T} \tag{4.10}$$

A linear plot with a negative slope can be established by plotting ln $({t_{0.5}}^{-1})$ as a function of $T_m^\circ/(T_c\Delta T)$. The nucleation parameter, K_g can then be obtained from the slope of the plot. Figure 4.15 shows a plot of ln $({t_{0.5}}^{-1})$ versus $T_m^\circ/(T_c\Delta T)$ for pure PEO.

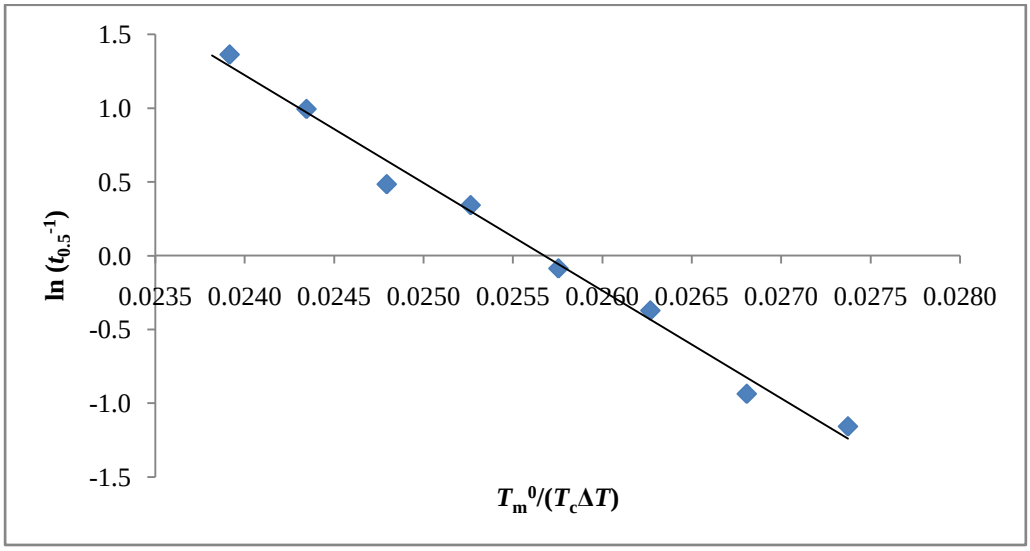

Figure 4.15: Plot of ln $({t_{0.5}}^{-1})$ versus $T_m^\circ/(T_c\Delta T)$ for pure PEO.

From the slope, the nucleation parameter, K_g of pure PEO was found to be 729.7 K. The high value of K_g obtained was attributed to the high molecular weight of PEO used (Huang, 2004).

Huang (2004) conducted a study to investigate the nucleation parameters, K_g of PEO with different molecular weights. The K_g of PEO with an average molecular weight of 75,000 g/mol and 157,000 g/mol was found to be 470.0 K and 520.6 K, respectively. The increase of K_g with increasing

molecular weight of PEO indicated that K_g of PEO was dependent on its molecular weight.

Table 4.3 shows the nucleation parameters, K_g for different blend compositions. It can be seen that the values of K_g for PEO in the blends were lower than that for pure PEO.

Table 4.3: Nucleation parameters, K_g for different blend compositions.

Blend composition (PEO/maleated starch)	Nucleation parameter, K_g (K)
100/0	729.7
80/20	136.0
70/30	269.6
50/50	261.0

4.2.5 Determination of the interaction parameter, χ_{12} of PEO/maleated starch blends

An understanding of the melting and crystallisation behaviour of a crystalline/amorphous polymer blend gives useful information regarding the miscibility and the interactions between the polymers. It is important to note that crystallisation in the blend does not indicate a phase separation in the polymer melt. In fact, miscibility can exist in the amorphous domains of the polymer as well as in the melt (Cesteros, et. al., 1989). This concept is admitted as a criterion for compatibility. In this study, the presence of the amorphous maleated starch resulted in a decrease in the equilibrium melting temperature, T_m° of PEO in the blend. The equilibrium melting depression of PEO was used

to calculate the polymer-polymer interaction parameter, χ_{12} based on the Nishi-Wang equation. The equilibrium melting temperatures, T_{m}° of the PEO/maleated starch blends were taken into account when estimating the magnitude of the interaction parameter (Al-Rawajfeh, Al-Salah and Al-Rhael, 2006).

The Nishi-Wang equation is given as follows:

$$\left(\frac{1}{T_{\mathrm{m}}^{\circ}\ (\mathrm{blend})}-\frac{1}{T_{\mathrm{m}}^{\circ}\ (\mathrm{PEO})}\right)=-\frac{Rv_1}{\Delta H^{\circ}v_2}\left[\frac{\ln\phi_1}{\mathrm{m}_1}+\left(\frac{1}{m_1}-\frac{1}{m_2}\right)+\chi_{12}{\phi_2}^2\right] \qquad (4.11)$$

where T_{m}° (blend) and T_{m}° (PEO) represent the equilibrium melting temperatures of PEO in the PEO/maleated starch blends and pure PEO, respectively; R is the universal gas constant, which is 8.314 J mol^{-1} K^{-1}; v_1 and v_2 denote the molar volumes of PEO and maleated starch, respectively; ΔH° is the heat of fusion of the perfectly crystallisable polymer per mole of repeating unit; ϕ_1 and ϕ_2 represent the volume fractions of PEO and maleated starch, respectively; m_1 and m_2 are the degrees of polymerisation of PEO and maleated starch, respectively; χ_{12} is the polymer-polymer interaction parameter. Both m_1 and m_2 are large for polymers with high molecular weights. As such, these terms can be neglected. The Nishi-Wang equation can then be rearranged to give Equation (4.12):

$$\left(\frac{1}{T_{\mathrm{m}}^{\circ}\ (\mathrm{PEO})}-\frac{1}{T_{\mathrm{m}}^{\circ}\ (\mathrm{blend})}\right)=\frac{Rv_1}{\Delta H^{\circ}v_2}\chi_{12}{\phi_2}^2 \qquad (4.12)$$

The polymer-polymer interaction parameters, χ_{12} for PEO/maleated starch blends were calculated based on Equation (4.12) and are tabulated in Table 4.4.

Table 4.4: Polymer-polymer interaction parameters, χ_{12} for different blend compositions.

Blend composition (PEO/maleated starch)	Polymer-polymer interaction parameter, χ_{12}
80/20	-18.3347
70/30	-5.9653
50/50	-2.1570

The negative values of the polymer-polymer interaction parameter, χ_{12} for the PEO/maleated starch blends indicated that the PEO/maleated starch blends were thermodynamically miscible in the melt. This could be attributed to the hydrophilic interaction between the hydroxyl (-OH) group located in the side chain of the maleated starch and the oxygen atom of the ether group of PEO (Pereira, et. al., 2010). From the table, it can also be observed that the polymer-polymer interaction parameter, χ_{12} became less negative with increasing maleated starch content. This implied that the compatibility between PEO and maleated starch decreased with increasing maleated starch content. Therefore, it was deduced that the polymer-polymer interaction parameter, χ_{12} was composition dependent.

CHAPTER 5

CONCLUSION

Sago starch was modified using maleic anhydride as the esterifying agent. Pyridine was employed as the catalyst. The incorporation of maleate group into starch was confirmed using Fourier Transform Infrared (FTIR) spectroscopy. The presence of an intense absorption band at 1739 cm^{-1} in the IR spectrum of maleated starch indicated the successful incorporation of the maleate group.

The degree of substitution (DS) of starch was determined using back-titration method. The effects of several reaction parameters on DS of starch were investigated. The parameters included amount of maleic anhydride, amount of pyridine, and reaction temperature. DS of starch was found to increase with increasing amount of maleic anhydride up to 1.5 equiv., while DS of starch increased with increasing amount of pyridine up to 0.6 equiv. DS of starch increased with increasing reaction temperature. Furthermore, it was observed that the DS of starch synthesised in the presence of pyridine was always higher compared to the one without pyridine for the whole range of reaction temperatures studied.

Maleated starch with the highest DS was used to blend with PEO. Different compositions of PEO/maleated starch blends were prepared by solution casting technique. The isothermal crystallisation behaviour of PEO in the PEO/maleated starch blends was studied using Differential Scanning

Calorimetry (DSC). The values of Avrami exponent, n_A obtained for all the PEO/maleated starch blends varied between 1.5 and 2.0, indicating the crystal growth geometry of PEO in the blends was two dimensional. For pure PEO and all PEO/maleated starch blends, it was observed that the half-time of crystallisation, $t_{0.5}$ increased exponentially with increasing crystallisation temperature, T_c. Apart from T_c, the isothermal crystallisation of PEO in the blend was also influenced by the blend composition. The crystallisation rate of PEO in the PEO/maleated starch blend increased with increasing maleated starch content up to 20 %. However, the crystallisation rate of PEO in the blend decreased when the amount of maleated starch added was more than 20 %.

The equilibrium melting temperatures, T_m° of pure PEO and PEO in the blends were estimated using the Hoffman-Weeks approach. The T_m° of pure PEO was estimated to be 91.2 ℃. A depression in the melting temperature of PEO was observed for all the PEO/maleated starch blends studied.

Negative values of the polymer-polymer interaction parameter, χ_{12} were obtained for the PEO/maleated starch blends. This indicated that the PEO/maleated starch blends were thermodynamically miscible in the melt. Furthermore, it was observed that the polymer-polymer interaction parameter, χ_{12} became less negative with increasing maleated starch content. This implied that the compatibility between PEO and maleated starch decreased with increasing maleated starch content.

REFERENCES

Ačkar, Đ., Babić, J., Jozinović, A., Miličević, B., Jokić, S., Miličević, R., Rajič, M. and Šubarić, D., 2015. Starch Modification by Organic Acids and Their Derivatives: A Review. *Molecules*, 20(10), pp. 19554-19570.

Alay, S. C. A. and Meireles, M. A. A., 2015. Physicochemical properties, modifications and applications of starches from different botanical sources. *Food Science and Technology (Campinas)*, 35(2), pp. 215-236.

Alger, M., 1996. *Polymer Science Dictionary*. [e-book] London: Chapman & Hall. Available at: Google Books <books.google.com> [Accessed 11 February 2017]

Al-Rawajfeh, A.E., Al-Salah, H. A. and Al-Rhael, I., 2006. Miscibility, Crystallinity and Morphology of Polymer Blends of Polyamide-6/Poly(β-hydroxybutyrate). *Jordan Journal of Chemistry*, 1(2), pp. 155-170.

Askeland, D. R. and Wright, W. J., 2015. *The Science and Engineering of Materials*. [e-book] United States of America: Cengage Learning. Available at: Google Books <books.google.com> [Accessed 04 April 2017]

Ayoub, A. S. and Rizvi, S. S. H., 2014. An Overview on the Technology of Cross-Linking of Starch for Nonfood Applications. *Journal of Plastic Film and Sheeting*, 25, pp. 25-45.

Back, D. M. and Schmitt, R. L., 2004. Ethylene Oxide Polymers. *Encyclopedia of Polymer Science and Technology*, 9, pp. 805-827.

Bertolini, A., 2009. *Starches: Characterization, Properties, and Applications*. [e-book] Boca Raton: CRC Press. Available at: Google Books <books.google.com> [Accessed 11 February 2017]

Biswas, A., Shogren, R. L., Kim, S. and Willet, J. L., 2006. Rapid preparation of starch maleate half-esters. *Carbohydrate Polymers*, 64(3), pp. 484-487.

Brown, W., Foote, C., Iverson, B. and Anslyn, E., 2008. *Organic Chemistry*. [e-book] United States of America: Cengage Learning. Available at: Google Books <books.google.com> [Accessed 05 April 2017]

Cesteros, L. C., Quintana, J. R., Fernandez, J. A. and Katime, I. A., 1989. Misibility of Poly(ethylene oxide) with Poly(N-vinyl pyrrolidone): DMTA abd DTA studies. *Journal of Polymer Science: Part B: Polymer Physics*, 27(13), pp. 2567-2576.

Chandran, C. S., Shanks, R. and Thomas, S., 2014. Polymer Blends. In: Chandran, C. S., Shanks, R. and Thomas, S., eds. *Nanostructured Polymer Blends*. Amsterdam: Elsevier. pp. 1-14.

Chen, Z., Hay, J. N. and Jenkins, M. J., 2013. The kinetics of crystallization of poly(ethylene terephthalate) measured by FTIR spectroscopy. *European Polymer Journal*, 49(6), pp. 1722-1730.

Chi, H., Xu, K., Xue, D., Song, C., Zhang, W. and Wang, P., 2007. Synthesis of dodecenyl succinic anhydride (DDSA) corn starch. *Food Research International*, 40(2), pp. 232-238.

Chuah, K. P., Gan, S. N. and Chee, K. K., 1998. Determination of Avrami exponent by differential scanning calorimetry for non-isothermal crystallization of polymers. *Polymer*, 40(1), pp. 253-259.

Chung, W. T., Yeh, W. J. and Hong, P. D., 2002. Melting Behavior of Poly(trimethylene terephthalate). *Journal of Applied Polymer Science*, 83(11), pp. 2426-2433.

Crompton, T. R., 2006. *Polymer Reference Book*. [e-book] United Kingdom: Rapra Technology Limited. Available at: Google Books <books.google.com> [Accessed 05 April 2017]

Cziple, F. A. and Marques, A. J. V., 2008. Biopolymers versus Synthetic Polymers. *Analele Universitatii "Eftimie Murgu"*, 15(1), pp. 125-132.

Dhevi, D. M., Prabu, A. A. and Pathak, M., 2014. Miscibility, crystallization and annealing studies of poly(vinylidene fluoride)/hyperbranched polyester blends. *Polymer*, 55(3), pp. 886-895.

Diop, C. I. K., Li, H. L., Xie, B. J. and Shi, J., 2011. Impact of the catalytic activity of iodine on the granule morphology, crystalline structure, thermal properties and water solubility of acetylated corn (*Zea mays*) starch synthesized under microwave assistance. *Industrial Crops and Products*, 33(2), pp. 302-309.

Eliasson, A. C. ed., 2004. *Starch in Food: Structure, Function and Applications*. [e-book] Boca Raton: CRC Press. Available at: Google Books <books.google.com> [Accessed 11 February 2017]

Fang, J. M., Fowler, P. A., Sayers, C. and Williams, P. A., 2004. The chemical modification of a range of starches under aqueous reaction conditions. *Carbohydrate Polymers*, 55(3), pp. 283-289.

Foreman, J. and Blaine, R.L., 1995. Isothermal crystallization made easy: a simple model and modest cooling rates. *ANTEC'95.*, *2*, pp.2409-2412.

Fouladi, E. and Nafchi, A. M., 2014. Effects of acid-hydrolysis and hydroxypropylation on functional properties of sago starch. *International Journal of Biological Macromolecules*, http://dx.doi.org/10.1016/j.ijbiomac.2014.05.013

Freire, E., Bianchi, O., Martins, J. N., Monteiro, E. E. C. and Forte, M. M. C., 2012. Non-isothermal crystallization of PVDF/PMMA blends processed in low and high shear mixtures. *Journal of Non-Crystalline Solids*, 358(18-19), pp. 2674-2681.

Gunatillake, P. A. and Adhikari, R., 2003. Biodegradable Synthetic Polymers for Tissue Engineering. *Eurropean Cells and Materials*, 5(1), pp. 1-16.

Höhne, G., Hemminger, W. F. and Flammersheim, H. J., 2013. *Differential Scanning Calorimetry*. [e-book] New York: Springer Science & Business Media. Available at: Google Books <books.google.com> [Accessed 05 April 2017]

Huang, Z., 2004. *Crystallization and Melting Behavior of Linear Polyethylene and Ethylene/Styrene Copolymers and Chain Length Dependence of Spherulitic Growth Rate for Poly(Ethylene Oxide) Fractions*. PhD. Virginia Tech.

Ikehara, T. and Nishi, T., 2000. Primary and secondary crystallization processes of poly(ϵ-caprolactone)/styrene oligomer blends investigated by pulsed NMR. *Polymer*, 41(21), pp. 7855-7864.

John, M. J. and Thomas, S. eds., 2012. *Natural Polymers: Composites*. [e-book] Great Britain: Royal Society of Chemistry. Available at: Google Books <books.google.com> [Accessed 11 February 2017]

Kačuráková, M. and Wilson, R. H., 2001. Developments in mid-infrared FT-IR spectroscopy of selected carbohydrates. *Carbohydrate Polymers*, 44(4), pp. 291-303.

Kalkar, A. K. and Deshpande, A. A., 2001. Kinetics of Isothermal and Non-isothermal Crystallization of Poly(butylene terephthalate)/Liquid Crystalline Polymer Blends. *Polymer Engineering and Science*, 41(9), pp. 1597-1615.

Kalkar, A. K., Deshpande, V. D. and Kulkarni, M. J., 2008. Isothermal Crystallization Kinetics of Poly(phenylene sulfide)/TLCP Composites. *Polymer Engineering and Science*, 49(2), pp. 397-417.

Karmakar, R., Ban, D. K. and Ghosh, U., 2014. Comparative study of native and modified starches isolated from conventional and nonconventional sources. *International Food Research Journal*, 21(2), pp. 597-602.

Ke, T. and Sun, X., 2003. Melting Behaviour and Crystallization Kinetics of Starch and Poly(lactic acid) Composites. *Journal of Applied Polymer Science*, 89(5), pp. 1203-1210.

Kocic, N., Lederhofer, S., Kretschmer, K., Bastian, M. and Heidemeyer, P., 2015. Nucleation Parameter and Size Distribution of Critical Nuclei for Nonisothermal Polymer Crystallisation: The Influence of the Cooling Rate and Filler. *Journal of Applied Polymer Science*, 132(6), pp. 1-15.

Lewicka, K., Siemion, P. and Kurcok, P., 2015. Chemical Modifications of Starch: Microwave Effect. *International Journal of Polymer Science*, http://dx.doi.org/10.1155/2015/867697

Li, X., 1985. Studies of the crystallization behavior in the crystalline/amorphous polymer blends: poly(ethylene oxide)/poly(methyl methacrylate) and poly(ethylene oxide)/poly(vinyl acetate). *Polymer Communications*, 3, pp. 280-288.

Namazi, H., Fathi, F. and Dadkhah, A., 2011. Hydrophobically modified starch using long-chain fatty acids for preparation of nanosized starch particles. *Scientia Iranica*, 18(3), pp. 439-445.

Nawawi, M.A., Sim, L. H. and Chan, C. H., 2012. Miscibility of Polymer Blends Comprising Poly(Ethylene Oxide) – Epoxidized Natural Rubber. *International Journal of Chemical Engineering and Applications*, 3(6), pp. 410-412.

Odian, G., 2004. *Principles of Polymerization*. [e-book] New Jersey: John Wiley & Sons. Available at: Google Books <books.google.com> [Accessed 11 February 2017]

Okeda, M., Ogawa, Y. and Matsumoto, N., 2006. Equilibrium Melting Temperature of Aliphatic Polyesters Using Model Compounds. *Polymer Journal*, 38(10), pp. 1089-1092.

Papageorgiou, G. Z. and Panayiotou, C., 2011. Crystallisation and melting of biodegradable poly(propylene suberate). *Thermochimica Acta*, 523(1-2), pp. 187-199.

Park, S. H., Lim, S. T., Shin, T. K., Choi, H. J. and Jhon, M. S., 2001. Viscoelasticity of biodegradable polymer blends of poly(3-hydroxybutyrate) and poly(ethylene oxide). *Polymer*, 42(13), pp. 5737-5742.

Pereira, A. G. B., Paulino, A. T., Rubira, A. F. and Muniz, E. C., 2010. Polymer-polymer miscibility in PEO/cationic starch and PEO/hydrophobic starch blends. *eXPRESS Polymer Letters*, 4(8), pp. 488-499.

Qiu, Z., Ikehara, T. and Nishi, T., 2003. Miscibility and crystallization in crystalline/crystalline blends of poly(butylene succinate)/poly(ethylene oxide). *Polymer*, 44(9), pp. 2799-2806.

Ravve, A., 2000. *Principles of Polymer Chemistry, Volume 1*. [e-book] New York: Kluwer Academic/Plenum Publishers. Available at: Google Books <books.google.com> [Accessed 11 February 2017]

Reiter, G. and Sommer, J. U. eds., 2008. *Polymer Crystallization: Observations, Concepts and Interpretations*. [e-book] Germany: Springer. Available at: Google Books <books.google.com> [Accessed 11 February 2017]

Ren, Y., Yang, R., Liu, X. and Liu, F., 2011. Study on miscibility of poly(vinyl chloride) and polyepichlorohydrin by viscometric and thermal analysis. *European Polymer Journal*, 47(10), pp. 2016-2021.

Shafee, E. E. and Ueda, W., 2002. Crystallization and melting behaviour of poly(ethylene oxide)/poly(*n*-butyl methacrylate) blends. *European Polymer Journal*, 38(7), pp. 1327-1335.

Sigma-Aldrich, 2017. *Amylases, α-Glucosidase, Starches (Amylose and Amylopectin) and Glycogen*. [electronic print] Available at: <http://www.sigmaaldrich.com/life-science/biochemicals/biochemical-products.html?TablePage=111642816> [Accessed 01 April 2017].

Sigma-Aldrich, 2017. *Poly(ethylene oxide)*. [electronic print] Available at: < http://www.sigmaaldrich.com/catalog/product/aldrich/181986?lang=en&region=MY> [Accessed 03 April 2017].

Sigma-Aldrich, 2017. *Pyridine, anhydrous, 99.8 %*. [electronic print] Available at: < http://www.sigmaaldrich.com/catalog/product/sial/270970?lang=en&region=MY> [Accessed 04 April 2017].

Soccio, M., Lotti, N., Finelli, L. and Munari, A., 2012. Equilibrium melting temperature and crystallization kinetics of α- and β'-PBN crystal forms. *Polymer Journal*, 44, pp. 174-180.

Soto, D., Urdaneta, J. and Pernia, K., 2014. Characterization of Native and Modified Starches by Potentiometric Titration. *Journal of Applied Chemistry*, http://dx.doi.org/10.1155/2014/162480

Sun, N. X., Liu, X. D. and Lu, K., 1996. An Explanation to the Anomalous Avrami Exponent. *Scripta Materialia*, 34(8), pp. 1201-1207.

Sun, R. and Sun, X. F., 2002. Succinoylation of sago starch in the *N*,*N*-dimethylacetamide/lithium chloride system. *Carbohydrate Polymers*, 47(4), pp. 323-330.

Tay, S. H., Pang, S. C. and Chin, S. F., 2012. Facile synthesis of starch-maleate monoesters from native sago starch. *Carbohydrate Polymers*, 88(4), pp. 1195-1200.

Thakur, V. K. and Kessler, M. R. eds., 2015. *Liquid Crystalline Polymers: Volume 1 – Structure and Chemistry*. [e-book] Switzerland: Springer. Available at: Google Books <books.google.com> [Accessed 06 April 2017]

Thomas, S., Grohens, Y. and Jyotishkumar, P., 2014. Polymer Blends: State of the Art, New Challenges, and Opportunities. In: S. Thomas, Y. Grohens and P. Jyotishkumar, eds., 2014. *Characterization of Polymer Blends: Miscibility, Morphology and Interfaces*. Weinheim: Wiley-VCH Verlag GmbH & Co. KGaA. pp. 1-5.

Wang, S. and Copeland, L., 2013. Molecular disassembly of starch granules during gelatinization and its effect on starch digestibility: a review. *Food & Function*, 4(11), pp. 1564-1580.

Wang, S., Li, C., Copeland, L., Niu, Q. and Wang, S., 2015. Starch Retrogradation: A Comprehensive Review. *Comprehensive Reviews in Food Science and Food Safety*, 14(5), pp. 568-585.

Whistler, R. L., BeMiller, J. N. and Paschall, E. F. eds., 2012. *Starch: Chemistry and Technology*. [e-book] London: Academic Press. Available at: Google Books <books.google.com> [Accessed 04 April 2017]

Wu, Y. P., Qi, Q., Liang, G. H. and Zhang, L. Q., 2006. A strategy to prepare high performance starch/rubber composites: In situ modification during latex compounding process. *Carbohydrate Polymers*, 65(1), pp. 109-113.

Zou, H., Wang, L., Yi, C. and Gan, H., 2011. Thermal properties and non-isothermal crystallization behaviour of poly(trimethylene terephthalate)/poly(lactic acid) blends. *Polymer International*, 60, pp. 1349-1354.

Zuo, Y. F., Gu, J., Qiao, Z., Tan, H., Cao, J. and Zhang, Y., 2015. Effects of dry method esterification of starch on the degradation characteristics of starch/ polylactic acid composites. *International Journal of Biological Macromolecules*, 72, pp. 391-402.

Zuo, Y., Gu, J., Yang, L., Qiao, Z., Tan, H. and Zhang, Y., 2013. Synthesis and characterization of maleic anhydride esterified corn starch by the dry method. *International Journal of Biological Macromolecules*, 62, pp. 241-247.

APPENDIX A

A.1 Data for degree of substitution of starch

A.1.1 Data for Figure 4.4

Amount of maleic anhydride (equiv.)	Degree of substitution
0.5	0.1230
1.0	0.2254
1.5	0.3837
2.0	0.3837
2.5	0.2470

A.1.2 Data for Figure 4.5

Amount of pyridine (equiv.)	Degree of substitution
0.0	0.0762
0.2	0.1106
0.4	0.1149
0.6	0.1371
0.8	0.1105
1.0	0.1019

A.1.3 Data for Figure 4.6

Reaction temperature (℃)	Degree of substitution
0.5 equiv. of pyridine	
70.0	0.0708
75.0	0.0902
80.0	0.1151
90.0	0.1230
100.0	0.1230
110.0	0.1230
No pyridine	
70.0	0.0230
75.0	0.0420
80.0	0.0612
90.0	0.0687
100.0	0.0762
110.0	0.0992

APPENDIX B

B.1 Degree of crystallinity, X_c for PEO/maleated starch blends

The degrees of crystallinity, X_c of PEO and PEO in the blends are calculated using the following equation:

$$X_c = \frac{\Delta H_m}{\Delta H_m^\circ \times w_{PEO}} \times 100\ \%$$

where ΔH_m denotes the melting enthalpy of PEO in the blend after isothermal crystallisation, J/g; ΔH_m° refers to the melting enthalpy of 100 % crystalline PEO, J/g; w_{PEO} is the weight fraction of PEO in the blend. ΔH_m° was taken to be 196.6 J/g from the literature.

B.1.1 Example of calculation of degree of crystallinity, X_c for pure PEO at crystallisation temperature, T_c = 46.0 °C

For pure PEO,

ΔH_m° = 196.6 J/g

ΔH_m = 126.84 J/g

w_{PEO} = 1.0

$$X_c = \frac{\Delta H_m}{\Delta H_m^\circ \times w_{PEO}} \times 100\ \%$$

$$= \frac{126.84\ \text{J/g}}{196.6\ \text{J/g} \times 1.0} \times 100\ \%$$

$$= 64.5\ \%$$

B.1.2 Data for Figure 4.7

Weight fraction of maleated starch	Degree of crystallinity, X_c (%)
0.0	64.5
0.1	62.1
0.2	66.6
0.3	62.4
0.4	48.6
0.5	51.0

APPENDIX C

C.1 Data for isothermal crystallisation of pure PEO and PEO in the PEO/maleated starch blends

C.1.1 Data for Figure 4.9

log [-ln(1-X_t)]	log (t-t_0)		
	44.0˚C	46.0˚C	48.0˚C
-1.2899	-0.9208	-0.5686	-0.4089
-0.9773	-0.7213	-0.3872	-0.2007
-0.7891	-0.6198	-0.2840	-0.0862
-0.6514	-0.5528	-0.2076	-0.0044
-0.5411	-0.4949	-0.1549	0.0569
-0.4477	-0.4437	-0.1024	0.1139
-0.3657	-0.4089	-0.0605	0.1614
-0.2917	-0.3665	-0.0223	0.2041
-0.2234	-0.3280	0.0128	0.2455
-0.1592	-0.3010	0.0492	0.2856
-0.0977	-0.2676	0.0828	0.3243
-0.0380	-0.2366	0.1139	0.3617
0.0211	-0.2007	0.1492	0.4014
0.0806	-0.1739	0.1847	0.4425
0.1419	-0.1367	0.2253	0.4871
0.2067	-0.0969	0.2718	0.5366
0.2781	-0.0506	0.3284	0.5977
0.3622	0.0212	0.4133	0.6785
0.4765	0.2810	0.5966	0.8261
0.5077	0.3927	0.6646	0.8797
0.5449	0.5132	0.7543	0.9513
0.5924	0.6513	0.8651	1.0457
0.6632	0.8156	1.0107	1.1632

C.1.2 Data for Figure 4.10

Crystallisation temperature, T_c (℃)	Half-time of crystallisation, $t_{0.5}$ (min)
43.0	0.352
44.0	0.500
45.0	0.570
46.0	1.120
47.0	1.390
48.0	1.930
49.0	3.980
50.0	6.862

C.1.3 Data for Figure 4.11

Crystallisation temperature, T_c (℃)	Generalised rate constant, K_A^{1/n_A}
43.0	2.33
44.0	1.61
45.0	1.37
46.0	0.71
47.0	0.59
48.0	0.40
49.0	0.19
50.0	0.12

C.1.4 Data for Figure 4.12

Crystallisation temperature, T_c (℃)	log ($t_{0.5}^{-1}$)	log (K_A^{1/n_A})
43.0	0.6017	0.4610
44.0	0.4567	0.3515
45.0	0.3565	0.2559
46.0	0.3279	0.2236
47.0	0.2007	0.0933
48.0	0.1592	-0.1167
49.0	-0.1072	-0.2145
50.0	-0.2878	-0.4035

C.1.5 Data for Figure 4.13

Weight fraction of maleated starch	Reciprocal of half-time of crystallisation, $t_{0.5}^{-1}$
T_c = 45.0˚C	
0.0	1.6234
0.1	1.6579
0.2	2.2727
0.3	2.1739
0.4	1.8519
0.5	1.7544
T_c = 46.0˚C	
0.0	1.4085
0.1	1.4566
0.2	2.1277
0.3	1.9231
0.4	1.1436
0.5	0.8929
T_c = 47.0˚C	
0.0	0.9174
0.1	1.4085
0.2	1.5873
0.3	1.2987
0.4	0.8341
0.5	0.7194

T_c = 48.0°C		
	0.0	0.6897
	0.1	0.8547
	0.2	1.4427
	0.3	0.7299
	0.4	0.5917
	0.5	0.5181
T_c = 49.0°C		
	0.0	0.3922
	0.1	0.7143
	0.2	0.7813
	0.3	0.4587
	0.4	0.2978
	0.5	0.2513
T_c = 50.0°C		
	0.0	0.3145
	0.1	0.4878
	0.2	0.5155
	0.3	0.2531
	0.4	0.1701
	0.5	0.1457

APPENDIX D

D.1 Data for the estimation of equilibrium melting temperature, T_m° of pure PEO and PEO in the PEO/maleated starch blends

D.1.1 Data for Figure 4.14

Crystallisation temperature, T_c (℃)	Observed melting temperature, T_m (℃)
100/0 PEO/maleated starch blend	
45.0	72.1
46.0	72.0
47.0	-
48.0	72.7
49.0	73.7
50.0	74.0
70/30 PEO/maleated starch blend	
45.0	62.3
46.0	62.7
47.0	63.0
48.0	63.3
49.0	64.0
50.0	64.3

50/50 PEO/maleated starch blend	
45.0	60.3
46.0	61.3
47.0	61.3
48.0	61.7
49.0	62.0
50.0	62.8

APPENDIX E

E.1 Data for the determination of nucleation parameter, K_g for isothermal polymer crystallisation

E.1.1 Data for Figure 4.15

$\ln (t_{0.5}^{-1})$	$T_m^\circ/(T_c\Delta T)$
1.3634	0.0239
0.9943	0.0243
0.4845	0.0248
0.3425	0.0253
-0.0862	0.0257
-0.3716	0.0263
-0.9361	0.0268
-1.1569	0.0274

APPENDIX F

F.1 Polymer-polymer interaction parameter, χ_{12} of PEO/maleated starch blend

The polymer-polymer interaction parameters, χ_{12} of PEO/maleated starch blends are calculated using the following equation:

$$\left(\frac{1}{T_{\mathrm{m}}^{\circ}\ (\mathrm{PEO})} - \frac{1}{T_{\mathrm{m}}^{\circ}\ (\mathrm{blend})}\right) = \frac{Rv_1}{\Delta H^{\circ} v_2}\chi_{12}{\phi_2}^2$$

where T_{m}° (blend) and T_{m}° (PEO) represent the equilibrium melting temperatures of PEO in the PEO/maleated starch blends and pure PEO, respectively; R is the universal gas constant, which is 8.314 J mol^{-1} K^{-1}; v_1 and v_2 denote the molar volumes of PEO and maleated starch, respectively; ΔH^{o} is the heat of fusion of the perfectly crystallisable polymer per mole of repeating unit; ϕ_2 represents the volume fraction of maleated starch.

F.1.1 Example of calculation of polymer-polymer interaction parameter, χ_{12} for 80/20 PEO/maleated starch blend

For 80/20 PEO/starch blend,

$$\left(\frac{1}{T_{\mathrm{m}}^{\circ}\ (\mathrm{PEO})}-\frac{1}{T_{\mathrm{m}}^{\circ}\ (\mathrm{blend})}\right)=\frac{Rv_1}{\Delta H^{\circ}v_2}\chi_{12}{\phi_2}^2$$

$T_{\mathrm{m}}{}^{\mathrm{o}}\ (\mathrm{PEO}) = 91.19\ ℃$

$= 364.19\ \mathrm{K}$

$T_{\mathrm{m}}{}^{\mathrm{o}}\ (\mathrm{blend}) = 69.10\ ℃$

$= 342.10\ \mathrm{K}$

$$\left(\frac{1}{T_{\mathrm{m}}{}^{\mathrm{o}}\ (\mathrm{PEO})}-\frac{1}{T_{\mathrm{m}}{}^{\mathrm{o}}\ (\mathrm{blend})}\right)=\left(\frac{1}{364.19\ \mathrm{K}}-\frac{1}{342.10\ \mathrm{K}}\right)$$

$$= -1.7730\times10^{-4}\ \mathrm{K}^{-1}$$

$\rho_{\mathrm{starch}} = 1.5\ \mathrm{g/cm^3}$

$\rho_{\mathrm{PEO}} = 1.09\ \mathrm{g/cm^3}$

$w_{\mathrm{starch}} = 0.2$

$${\phi_2}^2=\left(\frac{w_{\mathrm{starch}}}{w_{\mathrm{starch}}+(1-w_{\mathrm{starch}})\left(\frac{\rho_{\mathrm{starch}}}{\rho_{\mathrm{PEO}}}\right)}\right)^2$$

$= 0.02364$

$\mathrm{R} = 8.314\ \mathrm{J\ mol^{-1}\ K^{-1}}$

$\Delta H^{\circ}(\mathrm{PEO}) = 7.6\ \mathrm{kJ\ mol^{-1}}$

$$v_1(\mathrm{PEO})=\frac{\text{molar mass of repeating unit}}{\text{denisty of polymer}}$$

$$=\frac{44.053\ \mathrm{g/mol}}{1.09\ \mathrm{g/cm^3}}$$

$$= 40.42\ \mathrm{cm^3/mol}$$

$$v_2(\text{starch}) = \frac{\text{molar mass of repeating unit}}{\text{denisty of polymer}}$$

$$= \frac{162.141\ \text{g/mol}}{1.5\ \text{g/cm}^3}$$

$$= 108.094\ \text{cm}^3/\text{mol}$$

$$\frac{\text{R}v_1}{\Delta H^\circ v_2} = 4.0906 \times 10^{-4}\ \text{K}^{-1}$$

$$\chi_{12} = \frac{\left(\frac{1}{T_\text{m}^{\ \text{o}}\ (\text{PEO})} - \frac{1}{T_\text{m}^{\ \text{o}}\ (\text{blend})}\right)}{\left(\frac{\text{R}v_1}{\Delta H^\circ v_2}\right)\left({\phi_2}^2\right)}$$

$$= \frac{-1.7730 \times 10^{-4}\ \text{K}^{-1}}{(4.0906 \times 10^{-4}\ \text{K}^{-1})(0.02364)}$$

$$= -18.3347$$